

# PET Tracers for Mapping Adenosine Receptors as Probes for Diagnosis of CNS Disorders

Kiichi Ishiwata<sup>1,\*</sup>, Yuichi Kimura<sup>1</sup>, Erik F.J. de Vries<sup>2</sup> and Philip H. Elsinga<sup>2</sup>

<sup>1</sup>Positron Medical Center, Tokyo Metropolitan Institute of Gerontology, 1-1, Naka, Itabashi, Tokyo, 173-0011, Japan;

<sup>2</sup>Dept. of Nuclear Medicine and Molecular Imaging, University Medical Center Groningen, University of Groningen, PO Box 30.001, 9700 RB, Groningen, The Netherlands

**Abstract:** Adenosine is an endogenous modulator of several physiological functions in the central nervous system (CNS). The effect is mediated by a receptor family that consists of at least four subtypes: A<sub>1</sub>, A<sub>2A</sub>, A<sub>2B</sub> and A<sub>3</sub> receptors. The adenosine receptors play a role in neurological and psychiatric disorders such as Alzheimer's disease, Parkinson's disease, epilepsy and schizophrenia. Knowledge on adenosine receptor densities and status are important for understanding the mechanisms underlying the pathogenesis of diseases and for developing new therapeutics. Positron emission tomography (PET) offers a non-invasive tool to investigate these features *in vivo*, provided that suitable radiopharmaceuticals are available.

As a consequence of the development of xanthine-type adenosine receptor antagonists with high affinity and high selectivity, several PET ligands labeled with carbon-11 (half-life of 20.4 min) and fluorine-18 (half-life of 109.8 min) have been proposed for mapping the adenosine A<sub>1</sub> and A<sub>2A</sub> receptors (A<sub>1</sub>R and A<sub>2A</sub>R, respectively) and the adenosine uptake site in the CNS since 1995. Later non-xanthine-type antagonists for A<sub>2A</sub>R were radiolabeled. So far two tracers for A<sub>1</sub>R, [<sup>18</sup>F]CPFPX and [<sup>11</sup>C]MPDX, and a tracer for A<sub>2A</sub>R, [<sup>11</sup>C]TMSX (also called [<sup>11</sup>C]KF18446), have been applied to humans. For the other subtypes and the adenosine uptake site no suitable radioligands have been developed yet.

This paper gives an overview of the current status on PET tracers for mapping adenosine receptors and the development of new compounds that may lead to new PET tracers.

**Keywords:** Adenosine receptor, radiolabeled ligand, positron emission tomography, xanthine.

## 1. INTRODUCTION

Adenosine is an endogenous modulator of a variety of physiological functions in the central nervous system (CNS) as well as in peripheral organs. The effect is mediated by the family of adenosine receptors, which are Gi/o-protein coupled receptors (coupled to ion channels, adenylyl cyclase or phospholipases) and consist of four subtypes designated A<sub>1</sub>, A<sub>2A</sub>, A<sub>2B</sub> and A<sub>3</sub> receptors (A<sub>1</sub>R, A<sub>2A</sub>R, A<sub>2B</sub>R and A<sub>3</sub>R, respectively) [1-4]. For the last two decades, the A<sub>1</sub>R and A<sub>2A</sub>R have been extensively studied biologically and pharmacologically. Increasing evidence emerges that A<sub>2B</sub>R and A<sub>3</sub>R may be affected in pathophysiological events, and manipulations of adenosine receptors influence sleep and arousal, cognition and memory, neuronal damage and degeneration, as well as neuronal maturation [5-8,10]. There is growing evidence that each receptor subtype could also be a promising therapeutic target for neurodegenerative diseases such as Alzheimer's disease and Parkinson's disease and for other neurological pathologies such as epilepsy, ischaemic brain disorders or sleep disorders, as well as in a wide range of peripheral diseases, including cardiac ischaemic diseases, renal failure, immune and inflammatory disorders and cancer

[6,8-14]. The adenosine uptake site is also proposed as a therapeutic target [12,15,16].

Many neuroreceptors have been visualized *in vivo* by positron emission tomography (PET) and single-photon emission computed tomography (SPECT) with the corresponding radioligands with high affinity and high selectivity. These techniques have been applied to evaluate physiological and pathophysiological states of the receptors in humans with and without neurological and psychiatric disorders [17-19].

PET is a non-invasive technique to measure metabolic and functional processes *in vivo* in a quantitative way. By administration of radiopharmaceuticals, PET uses naturally occurring radionuclides that enable to prepare biologically active compounds in labeled form, so without affecting its properties by structural changes. The distribution throughout the body of the PET-radiopharmaceuticals can externally be measured in the tissues of interest as a function over time. Very useful for this purpose is <sup>11</sup>C. The use of the radionuclide <sup>18</sup>F (atom radius is comparable to a hydrogen atom) is an alternative in several cases. Radioactive half-lives of the most commonly used isotopes <sup>11</sup>C, <sup>13</sup>N, <sup>15</sup>O and <sup>18</sup>F are short, being 20, 10, 2 and 110 min, respectively. Therefore, repeated studies within a short time span are possible. Synthetic procedures for radiopharmaceuticals have to be rapid and a medical cyclotron and radiochemistry laboratory are required. The injected quantity (as expressed in mass units)

\*Address correspondence to this author at the Positron Medical Center, Tokyo Metropolitan Institute of Gerontology, 1-1, Naka, Itabashi, Tokyo, 173-0011, Japan; Tel: +81-3-3964-3241; Fax: +81-3-3964-2188; E-mail: ishiwata@pet.tmig.or.jp

of PET-tracers is very low (in the nanomolar range). Using these subpharmacological doses offers the possibility that highly potent compounds may be injected without any pharmacological effects. With PET, 3D-images are acquired yielding quantitative information on the distribution of the PET-tracers as a function of time. Spatial resolution for clinical PET-cameras is in the range of 4-8 mm, whereas this resolution for animal PET-scanners is 0.5-2 mm. To account for the fate of the tracer, kinetic modeling is applied. The tracer can either be free, or bound (specific or non-specific) or can be metabolized. Tracer kinetic modeling is a mathematical description of the fate of the tracer in the human body over time. Using PET, it is possible to measure parameters, such as enzyme activity, biosynthesis rate, and receptor density/occupancy.

In addition, PET is increasingly used as a tool in CNS drug discovery and development or evaluation of the efficacy of drugs [20]. PET assessment of the adenosine receptor system in the CNS probably offers us a new diagnostic tool for neurological and psychiatric disorders as well as an opportunity to understand the general neurotransmission system more profoundly. The early work on developing PET tracers for the adenosine receptor has been reviewed previously [21-23]. This paper describes an overview of the current status of the development of PET radioligands for mapping adenosine receptors and the development of new lead compounds for potential PET radioligands.

## 2. POST-MORTEM HUMAN BRAIN STUDIES ON ADENOSINE RECEPTORS

A limited number of studies of the postmortem human brains have been reported for the A<sub>1</sub>R and A<sub>2A</sub>R adenosine receptors by both membrane and *in vitro* autoradiographic receptor binding methods, but not for A<sub>2B</sub>R and A<sub>3</sub>R. First distribution of A<sub>1</sub>R was quantitatively assayed by Fastbom *et al.* [24]. Later, Svenningsson quantitatively visualized distribution of A<sub>1</sub>R and A<sub>2A</sub>R in whole-hemisphere sections [25,26]. A<sub>1</sub>R were widely distributed, with the highest densities in the striatum radiatum/pyramidale of the hippocampal region CA1. Jennings *et al.* found co-localization of adenosine uptake sites and A<sub>1</sub>R [27], while Glass *et al.* reported slightly different distribution patterns in the hippocampus [28]. On the other hand, A<sub>2A</sub>R were abundant in the putamen, nucleus caudatus, nucleus accumbens, and globus pallidus pars lateralis, and were also found in certain thalamic nuclei and throughout the cerebral cortex.

In patients with Alzheimer's disease, density of A<sub>1</sub>R was reduced in the hippocampus [29-32]. However, the reduction was also observed in other types of dementia and was devoid of the specificity for Alzheimer's disease [33]. The decreased density of A<sub>1</sub>R was also observed in the caudate and putamen [34]. In patients suffering from temporal lobe epilepsy, upregulation of A<sub>1</sub>R (48% increase) was found in the neocortex by Angelatou *et al.* [35], while Glass *et al.* found that the A<sub>1</sub>R were reduced in epileptic temporal cortex [36].

As for A<sub>2A</sub>R, in patients with Huntington's disease in which selective degeneration of the striatopallidal neurons is one of the pathological features, the density of A<sub>2A</sub>R is significantly reduced in the striatum [37,38]. The loss of A<sub>2A</sub>R

in the caudate nucleus, putamen and external globus pallidus was more predominant than that of dopamine D<sub>2</sub> receptor binding [38]. In patients with Parkinson's disease characterized by selective degeneration of nigrostriatal dopamine neurons, the density of A<sub>2A</sub>R is not significantly affected [37]. In patients with schizophrenia, Kurumaji and Toru found a significant increase in the A<sub>2A</sub>R in the caudate and putamen [39]. However, Deckert *et al.* reported that antipsychotic medication induced upregulation of striatal A<sub>2A</sub>R [40].

There are several limitations in the postmortem studies of brain disorders. The effect of tissue perfusion is excluded. The good preservation of the tissues is essential to avoid autolysis and the duration preserving the tissues may alter the findings. Furthermore, the progress of brain disorders cannot be followed in the same subjects. From these points of view, PET evaluation of the brain disorders has a much advantage for pathophysiological studies.

## 3. ADENOSINE A<sub>1</sub> RECEPTOR LIGANDS

Adenosine presynaptically inhibits the release of many neurotransmitters, especially excitatory ones such as the potentially excitotoxic amino acid glutamate. This effect of adenosine is mediated by presynaptic A<sub>1</sub>R linked via G-proteins to both calcium and potassium ion channels. Thus, A<sub>1</sub>R inhibit neuronal communication, and are the potential therapeutic target for neurodegenerative diseases such as Alzheimer's disease and for other neurological situation such as epilepsy. A large numbers of potent A<sub>1</sub>R agonists and antagonists with high affinity and high selectivity have been developed and reviewed [41-45]. Cyclohexyladenosine, an adenosine agonist, and other related nucleosides have high and selective affinity for A<sub>1</sub>R, and [<sup>3</sup>H]cyclohexyladenosine has been used *in vitro* as a standard radioligand for A<sub>1</sub>R [24,28,29,34]. However, they are not appropriate ligands *in vivo* because of the low penetration of the blood-brain barrier. On the other hand, xanthine derivatives such as DPCPX [46,47] and KF15372 [48,49] are candidates for use as *in vivo* tracer for mapping the A<sub>1</sub>R in CNS. [<sup>3</sup>H]DPCPX has been used *in vitro* as a radioligand with high and A<sub>1</sub>-selective affinity [25,31-33]. Several PET ligands derived from xanthine derivatives have been evaluated (Fig. 1, Table 1) and two of them have been used in clinical studies up to now. Recently, a nonxanthine-type PET ligand has been prepared from pyrazolopyridine analogs [50].

### 3.1. PET Ligands

Ishiwata *et al.* proposed [<sup>11</sup>C]KF15372 as a PET probe for the A<sub>1</sub>R [54,55]. The corresponding despropyl precursor was labeled using [<sup>11</sup>C]propyl iodide with a relatively low radiochemical yield of 5% based on [<sup>11</sup>C]propyl iodide. [<sup>11</sup>C]KF15372 showed promising characteristics in rodents *in vivo*: reversible and receptor-specific uptake (70-80%) into the brain and a regional distribution pattern in the brain which was consistent with the distribution pattern of A<sub>1</sub>R *in vitro*. They further found that the [<sup>11</sup>C]ethyl and [<sup>11</sup>C]methyl analogs ([<sup>11</sup>C]EPDX and [<sup>11</sup>C]MPDX, respectively) of [<sup>11</sup>C]KF15372 are also candidates for PET probes [56]. Among these three PET-ligands, [<sup>11</sup>C]MPDX was prepared in a high radiochemical yield (20-30% based on [<sup>11</sup>C]methyl

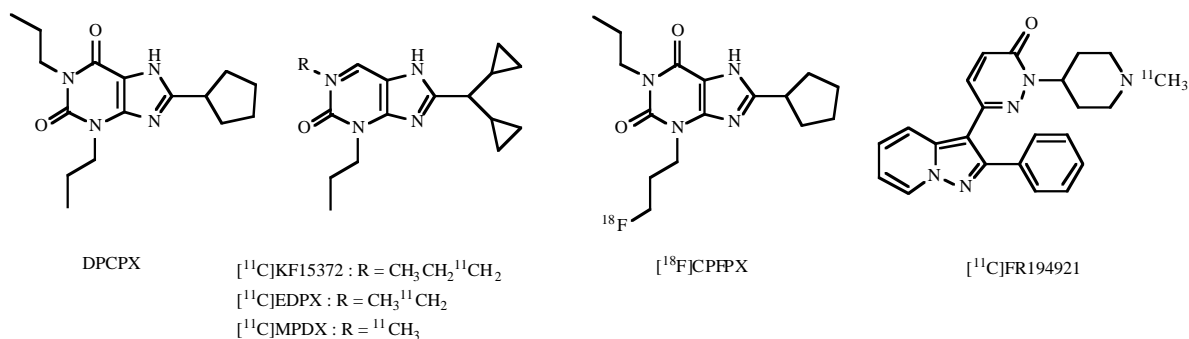


Fig. (1). PET ligands for the adenosine  $A_1$  receptor

Table 1. Binding Affinities of Adenosine  $A_1$  Receptor Ligands

	Affinity ( $K_i$ , nM)		Selectivity $A_{2A}/A_1$	Reference
	$A_1$	$A_{2A}$		
DPCPX	3.0	60	20	[52]
KF15372	3.0	430	143	[48]
EPDX	1.7	>100	>59	[56]
MPDX	4.2	>100	>24	[56]
CPFPX	0.183	812	4440	[63]
	$K_d$ : 0.63-1.37	$K_d$ : 940	>700	[64]
FR194921	2.9			[67]

iodide) and could easily penetrate the blood-brain barrier. In PET imaging studies of the cat and monkey brains, the levels of radioactivity of  $[^{11}\text{C}]\text{KF15372}$  and  $[^{11}\text{C}]\text{MPDX}$  reached a maximum at 10 min and 5 min, respectively.  $[^{11}\text{C}]\text{MPDX}$  levels decreased slightly faster than  $[^{11}\text{C}]\text{KF15372}$  due to its low affinity for  $A_1$ Rs [21,22,57,58]. The highest level of  $[^{11}\text{C}]\text{MPDX}$  [standardized uptake value (SUV, radioactivity/mL tissue  $\times$  g body weight/total injected radioactivity) was 3–5] was approximately twice that of  $[^{11}\text{C}]\text{KF15372}$  (SUV = 2–2.5), suggesting again that penetration of  $[^{11}\text{C}]\text{MPDX}$  into the brain is easier than that of  $[^{11}\text{C}]\text{KF15372}$ . The images of the two radioligands displayed a similar tracer distribution, which corresponds well with the regional distribution of  $A_1$ Rs. Furthermore, an *ex vivo* autoradiography study applying  $[^{11}\text{C}]\text{MPDX}$  to the rat model, in which monocular enucleation was done to destroy the anterior visual input, detected degeneration of the receptors [59], and a PET study applying  $[^{11}\text{C}]\text{MPDX}$  in a cat model demonstrated that  $[^{11}\text{C}]\text{MPDX}$  could be a good indicator of severe cerebral ischemic insult [60,61]. Thus, after preclinical studies including dosimetry and toxicology [62],  $[^{11}\text{C}]\text{MPDX}$  was moved further to clinical studies.

Holschbach *et al.* examined a series of xanthine compounds based on DPCPX as a leading compound for developing radioligands for PET and SPECT, and found several candidates containing iodine or fluorine [63]. From these series, they prepared  $[^{18}\text{F}]\text{CPFPX}$  by nucleophilic substitu-

tion with  $[^{18}\text{F}]\text{fluoride}$  with a high radiochemical yield of 45% [64], and found that  $[^{18}\text{F}]\text{CPFPX}$  showed high receptor-specific uptake (70–80%) in the brain of rodents *in vivo* [64,69]. In a glioma bearing rat model, Bauer *et al.* found that the binding of  $[^{18}\text{F}]\text{CPFPX}$  was increased in a zone surrounding tumors (136%–146% as compared to control brain tissue) due to upregulation of  $A_1$ R in activated astrocytes [65]. Furthermore in a preliminary study, the group demonstrated  $A_1$ R occupancy by caffeine in the rat brain by PET with  $[^{18}\text{F}]\text{CPFPX}$  [66].

Recently, Matsuya *et al.* proposed  $[^{11}\text{C}]\text{FR194921}$ , a highly selective, nonxanthine-type  $A_1$ R antagonist [67]. The tracer was prepared with a high radiochemical yield (38% based on  $[^{11}\text{C}]\text{methyl iodide}$ ), and showed receptor-specific uptake (50%) in the brain of rats *in vivo*. In PET imaging studies of the monkey brain, the images were similar to those of  $[^{11}\text{C}]\text{MPDX}$  (SUV = 3.05–3.5) [62], but the radioactivity accumulated for 60 min (SUV = 0.5–0.7, calculated assuming the body weight of the monkeys to be 4–5 kg) and then slightly decreased, suggesting that the affinity for  $A_1$ Rs may be too high for imaging in the time-frame of the PET scan using a  $^{11}\text{C}$ -labeled tracer (60–90 min).

The other radioligand labeled with positron emitter was 5'-(methyl $[^{75}\text{Se}]\text{seleno}$ )- $N^6$ -cyclopentyladenosine ( $^{75}\text{Se}$ , half life of 7.1 h) [68], but the biological evaluation of the tracer has not been reported.

### 3.2. Clinical Studies

In 2003 two groups visualized A<sub>1</sub>Rs in the human brain by PET using [<sup>18</sup>F]CPFPX [69] and [<sup>11</sup>C]MPDX [70,71]. For [<sup>18</sup>F]CPFPX, the validity as a ligand for A<sub>1</sub>Rs was investigated by comparing postmortem autoradiography [69] and then using a displacement study with cold CPFPX [72]. The spatial distribution of [<sup>11</sup>C]MPDX differed from regional cerebral blood flow ([<sup>15</sup>O]H<sub>2</sub>O PET) and regional cerebral metabolism of glucose ([<sup>18</sup>F]FDG PET), and the clinical possibility of [<sup>11</sup>C]MPDX was concluded. The affinity of [<sup>18</sup>F]CPFPX for A<sub>1</sub>Rs was higher than that of [<sup>11</sup>C]MPDX (Table 1); however, the latter was much more stable metabolically in humans than the former [71,73]. Thus, two tracers showed almost same potential for visualization of A<sub>1</sub>Rs. Fully quantitative methods to qualify the density of A<sub>1</sub>Rs was proposed for [<sup>11</sup>C]MPDX [74], and for [<sup>18</sup>F]CPFPX [75,76]. To efficiently perform PET clinical studies in patients with brain disorders, a non-invasive quantitative method without any blood sampling was further proposed for [<sup>11</sup>C]MPDX [77], as well as a simplified method based on venous blood sampling [<sup>18</sup>F]CPFPX [78].

### 3.3. Pharmacokinetic Modeling

#### 3.3.1. Compartmental Analysis for Radioligands

A ligand carried by blood flow enters into a brain tissue by perfusion through the capillary wall. Then, a part of the ligand in tissue binds to and dissociates from the receptor sites dynamically. Since PET measures a total amount of ligand in tissues that contain both unbound and bound ligands, some analytical approaches should be incorporated to determine receptor binding.

The behavior of ligand in tissues can be described using a compartmental model as shown in Fig. (2) [79,80]. In the model,  $C_p$  represents concentrations of the ligand in arterial plasma, and  $C_f$  and  $C_b$  denote unbound and specifically bound ligand to a target receptor site, respectively. The blood-brain barrier (BBB) is located between  $C_p$  and  $C_f$ . Ligand transportation from capillary to tissues is described with  $K_1$  [mL/min/g] containing a regional blood flow and permeability-surface product.  $k_2$  [1/min] represents the clearance rate back to venous blood.  $k_3$  [1/min] is a product of an association rate of a ligand to a receptor and a receptor-density ( $B_{max}$ ), and  $k_4$  [1/min] is equal to a disassociation

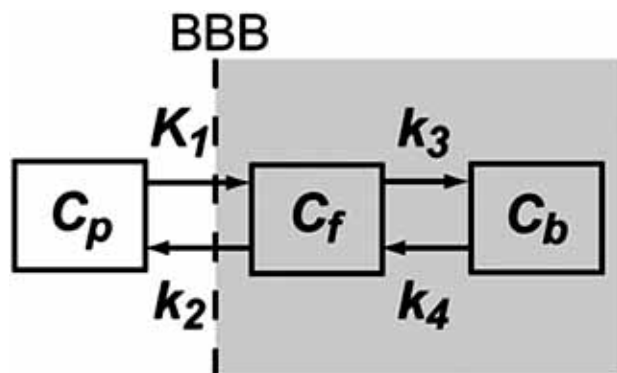


Fig. (2). Compartment model describing the behavior of an administered ligand.

rate. Mathematically it is difficult to estimate  $B_{max}$ . Instead, a binding potential ( $B_p$ ) defined as  $k_3/k_4$  is utilized for quantification of a receptor density which corresponds to  $B_{max}/K_D$ , the ratio of the association and disassociation rate of a ligand.

In kinetic analysis,  $B_p$  is estimated from the dynamic PET data  $C$  that is the sum of  $C_f + C_b$  and concurrently performed arterial blood sampling to derive  $C_p$ . But, the estimation is a nonlinear optimization problem, which is not easy to do, and the calculation speed is slow. Therefore, a graphical approach of the Logan plot is usually employed.

#### 3.3.2. Logan Plot

A Logan plot [81] is a simple and effective algorithm for receptor imaging. The operational equation of the Logan plot is obtained by integrating differential equations related to the compartment model; mathematical details are found in the equations (1) to (4) in [81]. As a summary, a linear relation is established between  $C$  and  $C_p$ :

$$\frac{\int_0^t C(u)du}{C(t)} = D_v \frac{\int_0^t C_p(u)du}{C(t)} + \beta \quad (\text{Eq.1})$$

$$D_v = \frac{K_1}{k_2} (1 + B_p) \quad (\text{Eq.2})$$

where the new quantity of  $D_v$  corresponds to a distribution volume. Logan showed that some minutes after the administration of ligand, the y-intercept,  $\beta$  becomes constant over time, and the slope of the plot gives  $D_v$  [82].

Then,  $B_p$  can be obtained from distribution volumes under the two assumptions: existence of a region in the brain where the receptors are ignorable, and  $K_1/k_2$  is common in whole brain. The region is referred as a reference region, and the cerebellum is a typical reference region for several neuroreceptors such as dopamine D<sub>2</sub> receptors. Under these assumptions,  $K_1/k_2$  is calculated as the distribution volume in the reference region, and  $B_p$  is computed as  $D_v/(D_v \text{ in the reference region}) - 1$ .

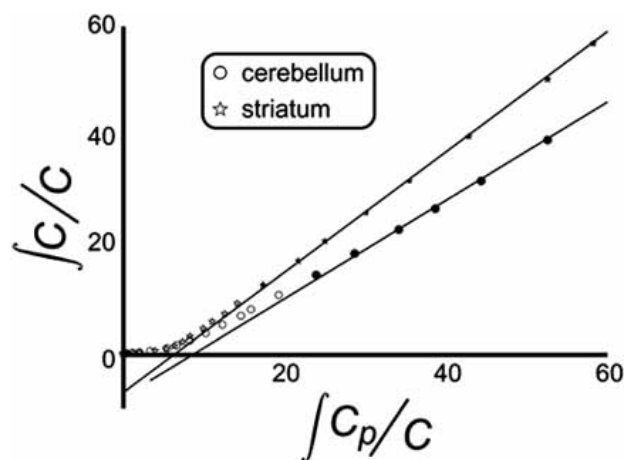
The Logan plot is fast and robust because it can be implemented as an estimation of a line, and so it is suitable for receptor imaging. However, it requires arterial blood sampling to obtain  $C_p$ . Arterial blood sampling requests an insertion of catheter into the brachial artery. This is sometimes painful and uncomfortable for patients, and has potential risks of infection, occlusion, bleeding, pseudoaneurysm, or thrombosis [83,84], thus it is preferable to omit arterial blood sampling for clinical situation. Some schemes were proposed: using predefined  $k_2$  [85], RPM in which mathematical reformulation is applied to the original compartmental model [86], and EPICA where a statistical approach is utilized to extract  $C_p$  from measured PET data [77,87].

A typical Logan plot is demonstrated in Fig. (3). It is derived from [<sup>11</sup>C]MPDX, and the slope in the striatum is larger than one in the cerebellum.

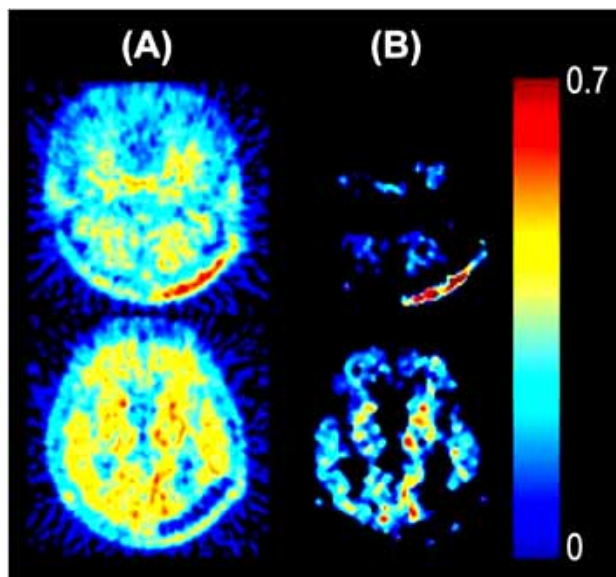
#### 3.3.3. Image of A<sub>1</sub>R

Fig. (4) demonstrates the effect of Logan graphical analysis applied to a case of a young normal subject with

[ $^{11}\text{C}$ ]MPDX [74]. In the static images, the contrast between cerebellum and major cortices is lower than those in the basal ganglia. The Logan graphical analysis clearly visualized a spatial distribution of the  $A_1$ Rs: low in the cerebellum and high in the basal ganglia which was reported in [24,25,69].



**Fig. (3).** Logan plot. It is derived from a dynamic [ $^{11}\text{C}$ ]MPDX PET scan of a normal young subject. At 20 min after tracer administration, a linear relationship is established. Cerebellum (circles) is an  $A_1$ R poor region, and striatum (star) is a receptor rich region. The slope of the plot reflects reversible receptor binding.



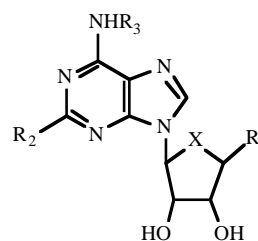
**Fig. (4).** Effect of Logan graphical analysis for adenosine  $A_1$  receptor using [ $^{11}\text{C}$ ]MPDX. Column (A) is a set of summed images of cross-sections of the cerebellum and the basal ganglia, and column (B) shows images of the  $Bp$  of the same cross-sections calculated by Logan plot graphical analysis.

### 3.4. Medicinal Chemistry

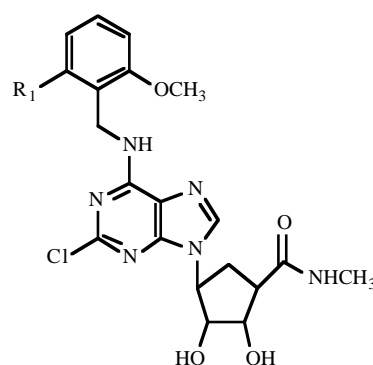
#### 3.4.1. $A_1$ Agonists

Several highly selective agonists for the  $A_1$ R have been developed [42-44]. As is shown in Fig. (5), all high affinity  $A_1$ R agonists have a chemical structure that is derived from

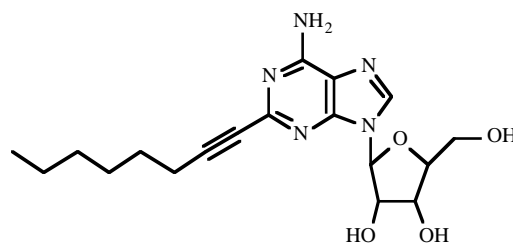
adenosine. Substitution at the  $N^6$  and C2 position of the adenine moiety is allowed and could increase sensitivity and subtype selectivity. The ribose ring in these compounds is crucial for agonist activity and only minor alterations that the 5'-hydroxyl group are tolerated.



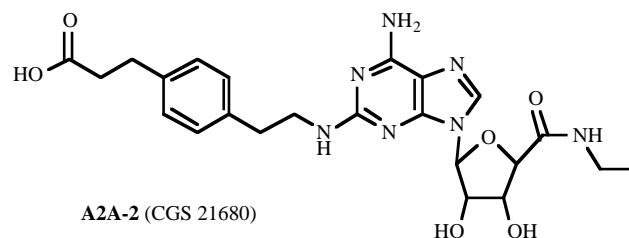
**A1-1a, -1b, -1c, -1d, -1e, -1f**  
**A3-1a, -1b, -1c, -1d**



**A3-2a, -2b, -2c**



**A2A-1 (YT-146)**



**A2A-2 (CGS 21680)**

**Fig. (5).** Adenosine receptor agonists.

Adenosine-5'-ethyluronamide (*N*-ethylcarboxamidoadenosine, NECA, **A1-1a**) is a 5'-substituted derivative of adenosine that is frequently used as an adenosine receptor agonist in binding assays. NECA can in principle be labeled with carbon-11 at the carbonyl group via an acylation reaction with [ $^{11}\text{C}$ ]propanoic chloride, in an analogous manner as described for [ $^{11}\text{C}$ ]WAY100635 [88]. However, [ $^{11}\text{C}$ ]NECA would not be a suitable PET tracer, because it lacks subtype selectivity (Table 2).

Table 2. Affinities and Subtype Selectivities of a Selection of Adenosine Receptor Agonists

Compound	R <sub>1</sub>	Substituents			LogP <sup>a</sup>	hA <sub>1</sub>	K <sub>i</sub> (nM)	hA <sub>3</sub>	Ref.
		R <sub>2</sub>	R <sub>3</sub>	X			hA <sub>2a</sub>		
<i>A<sub>1</sub> selective</i>									
<b>A1-1a</b> (NECA)	CONHEt	H	N	O	-0.5	14	16	49	[90]
A1-1b	2-FPhOCH <sub>2</sub>	H	3-THF <sup>b</sup>	O	1.7	12.7			[89]
<b>A1-1c</b> (CPA)	CH <sub>2</sub> OH	H	Cp <sup>b</sup>	O	1.0	0.30	385	26	[90]
<b>A1-1d</b> (CCPA)	CH <sub>2</sub> OH	Cl	Cp <sup>b</sup>	O	2.1	0.35	580	30	[90]
<b>A1-1e</b> ( <i>R</i> -PIA)	CH <sub>2</sub> OH	H	( <i>R</i> )- CH <sub>3</sub> CHCH <sub>2</sub> Ph	O	1.9	0.6	750	53	[90]
A1-1f	CH <sub>2</sub> OH	2- MeOPhNHCON HN=N	H	O	-1.0	20	125	81	[91]
<i>A<sub>2A</sub> selective</i>									
<b>A2A-1</b> (YT-146)					1.5	211	12.1		[172]
<b>A2A-2</b> (CGS 21680)					0.2	>10000	51.3		[137]
<i>A<sub>3</sub> selective</i>									
<b>A3-1a</b> (IB-MECA)	CONHCH <sub>3</sub>	H	3-IPhCH <sub>2</sub>	O	2.1	20		4.4	[151]
<b>A3-1b</b> (Cl-IB-MECA)	CONHCH <sub>3</sub>	Cl	3-IPhCH <sub>2</sub>	O	3.1	99		14	[151]
<b>A3-1c</b>	CONHCH <sub>3</sub>	Cl	3-IPhCH <sub>2</sub>	S	3.1	193	223	0.38	[152]
<b>A3-1d</b> (LJ530)	CONHCH <sub>3</sub>	Cl	CH <sub>3</sub>	S	0.5	1330		0.28	[152]
<b>A3-2a</b>	OCH <sub>3</sub>			O	0.8	1600		1.4	[153]
A3-2b	Cl			O	1.5	240	1200	1.5	[153]
<b>A3-2c</b>	I			O	2.1	200	430	0.58	[153]

<sup>a</sup> Calculated logP values were retrieved from the SciFinder<sup>®</sup> Scholar database, version 2004.2 (American Chemical Society). <sup>b</sup> Abbreviations: 3-THF: 3-tetrahydrofuryl; Cp: Cyclopentyl.

Morrison and coworkers described a series of 5'-aromatic ethers and sulfides as potential A<sub>1</sub>R selective agonist [89]. Among these compounds, **A1-1b**, with a 2-fluorophenyl group at the 5'-position and a tetrahydrofuryl moiety at N<sup>6</sup>, potentially could be converted into a PET tracer. It has a fairly high affinity for the A<sub>1</sub>R ( $K_i = 12.7$  nM), a favorable lipophilicity for brain penetration and an elimination half-life of 0.3 h, but its affinity for the other adenosine receptor subtypes is still unknown. Although compound **A1-1b** could - in theory - be labeled at the fluorophenyl group with high specific activity fluorine-18, this might prove difficult because the aromatic ring is not activated by electron withdrawing substituents that could facilitate a nucleophilic substitution reaction. Another drawback of compound **A1-1b** is that it shows some metabolism *in vivo*, resulting in formation of a

high affinity full agonist after cleavage of the fluorophenyl group.

The N<sup>6</sup>-substituted adenosine derivatives CPA (**A1-1c**), CCPA (**A1-1d**) and *R*-PIA (**A1-1e**) are well-known A<sub>1</sub>R agonists with sub-nanomolar affinity, high subtype selectivity and appropriate lipophilicity [90]. Unfortunately, these compounds do not appear to have any positions that can be easily labeled with a positron-emitting isotope.

Beukers *et al.* investigated a series of adenosine derivatives that are substituted at the C2 position with various aminocarbonyltriazene groups [91]. In this series, labeling of agonist **A1-1f** at the methoxy group by methylation with [<sup>11</sup>C]methyl iodide or [<sup>11</sup>C]methyl triflate seems feasible. However, the compound will probably not be suitable as a

PET tracer, because its affinity and selectivity are insufficient. Moreover, compound **A1-1f** is probably not able to penetrate into the brain, as it was calculated to have a logP value of  $-1.0$ .

Thus, none of the available agonists appears to have favorable properties for a PET tracer for A<sub>1</sub>R imaging.

### 3.4.2. A<sub>1</sub> antagonists

A considerable number of A<sub>1</sub>R antagonists has been developed in the past decades, some of which may be converted into promising PET tracers. In Fig. (6), a selection of potent A<sub>1</sub>R antagonists that can be labeled with carbon-11 is depicted. The A<sub>1</sub>R antagonists usually contain a polyheterocyclic core, but lack the ribose moiety that is essential for A<sub>1</sub>R agonists.

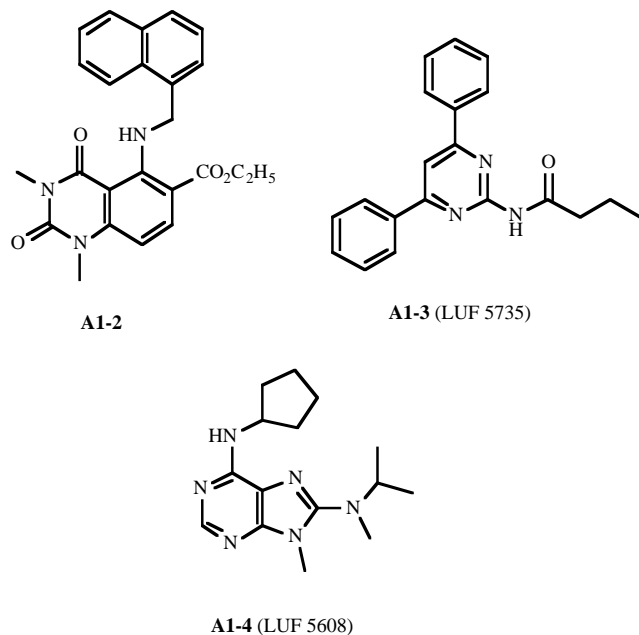


Fig. (6). Adenosine A<sub>1</sub> receptor antagonists.

The xanthine derivative DPCPX (Fig. 1) is probably the best-known potent A<sub>1</sub>R antagonist. It displays a 20 and 60-fold selectivity for the human A<sub>1</sub>R subtype over the A<sub>2A</sub>R and A<sub>3</sub>R subtypes, respectively [52]. A possible drawback of DPCPX could be its relatively high lipophilicity, which may give rise to high levels of nonspecific binding. Bisserbe *et al.* first reported the potential of DPCPX as a PET probe for labeling A<sub>1</sub>Rs [51]. It displays a 20 and 60-fold selectivity for the human A<sub>1</sub>R subtype over the A<sub>2A</sub>R and A<sub>3</sub>R subtypes, respectively (Fig. 1, Tables 1 and 2) [52]. They used the tritiated DPCPX and found that it exhibited preferable characteristics for a PET probe such as receptor-specific binding. The compound can potentially be labeled by alkylation using [<sup>11</sup>C]propyl iodide [53]; however, they did not advance further studies.

Bulicz *et al.* described a number of pyrido[2,3-d]pyrimidinediones as candidate A<sub>1</sub>R antagonists, of which compound **A1-2** displayed highest potency and good A<sub>1</sub>/A<sub>3</sub> selectivity. Likewise, LUF5735 (**A1-3**) was presented as the most potent antagonist in a series of pyrimidine derivatives [92]. Compounds **A1-2** and **A1-3** can be transformed into

PET tracers by [<sup>11</sup>C]methylation of an *N*-methyl substituent and by [<sup>11</sup>C]acylation at the amide function, respectively. Unfortunately, both compounds appear unsuitable as PET tracers, because of their high lipophilicity, causing a high extent of non-specific binding.

Among a series of substituted *N*<sup>6</sup>-cyclopentyl-adenine derivatives that were tested as antagonists for the A<sub>1</sub>R, LUF5608 (**A1-4**) displayed highest affinity [95]. The compound seems to have an acceptable logP of 2.9 and seems to be readily labeled by *N*-methylation. When the intrinsic activity of the compounds was determined in a [<sup>35</sup>S]GTPγS binding assay in CHO cells expressing the human A<sub>1</sub>R at high density, LUF5608 and DCPCX proved to be an inverse agonist instead of a neutral antagonist.

### 3.4.3. A<sub>1</sub> Allosteric Enhancers

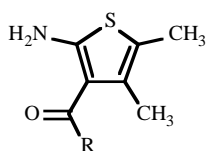
Allosteric enhancers of the adenosine receptor are compounds that augment the response of the receptor to adenosine or other agonists by stabilizing the agonist-receptor-G protein complex [20]. Consequently, the rate of dissociation of the agonist from the complex is reduced. Moreover, allosteric enhancers were suggested to stabilize the active conformation of the receptor even in the absence of an agonist. There is evidence that the A<sub>1</sub>R contains an allosteric binding site that is distinct from the agonist binding site [93]. PET imaging with radiolabeled allosteric enhancers may provide valuable information on the mode of action of these compounds. In this way the interaction of the allosteric enhancers with agonists can be measured using competition studies.

The thiophene derivative PD 81,723 (Fig. 7, **A1-5a**) was among the first A<sub>1</sub>R selective allosteric enhancers to be discovered [20]. This enhancer, however, also displayed antagonistic properties and therefore is not suited as a PET tracer. Baraldi and coworkers synthesized a series of naphthyl derivatives of PD 81,723 [93]. In this series, compound **A1-5b** was the only representative with allosteric activity that could easily be labeled by [<sup>11</sup>C]methylation of the methoxy substituent. Unfortunately, **A1-5b** is too lipophilic for a suitable PET tracer (logP 5.5).

Chordia *et al.* described a selection of 6-arylideno[1,2-d]thiazoles with allosteric enhancer activities in the low micromolar to sub-micromolar range [96]. The representatives **A1-6a**, **A1-6b** and **A1-6c** exhibited more than 4-fold greater allosteric enhancement activity than PD 81,723, with an EC<sub>50</sub> that ranged from 0.9 to 2.2 μM. The free bases of these compounds, however, show only minor allosteric enhancement activity. In contrast to PD81,723, these compounds displayed only weak A<sub>1</sub> and A<sub>3</sub> antagonistic activity. The compounds are stable towards oxidation in DMSO solution for months and their chemical structures allow labeling by [<sup>11</sup>C]methylation at oxygen or nitrogen. Thus, radiolabeled allosteric enhancers **A1-6a**, **A1-6b** and **A1-6c** warrant further investigation as PET tracers for the A<sub>1</sub>R allosteric binding site.

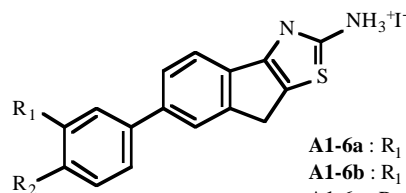
## 4. ADENOSINE A<sub>2A</sub> RECEPTOR LIGANDS

A<sub>2A</sub>Rs coupled with G-proteins exhibit a lower affinity to adenosine and enhance neuronal communication. They are restrictively distributed in the basal ganglia, particularly abundant in the striatum, which are thought to play a crucial role

**A<sub>1</sub> allosteric enhancers**

**A1-5a** : R = 3-CF<sub>3</sub>Ph (PD 81,723)

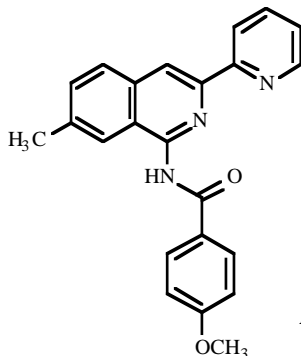
**A1-5b** : R = 1-(4-CH<sub>3</sub>O-naphtyl)



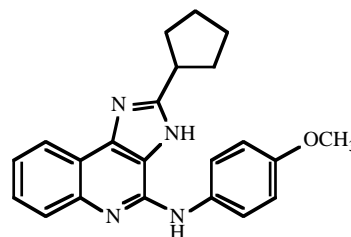
**A1-6a** : R<sub>1</sub> = OCH<sub>3</sub> ; R<sub>2</sub> = OCH<sub>3</sub>

**A1-6b** : R<sub>1</sub> = OCH<sub>3</sub> ; R<sub>2</sub> = H

**A1-6c** : R<sub>1</sub> = N(CH<sub>3</sub>)<sub>2</sub> ; R<sub>2</sub> = H

**A<sub>3</sub> allosteric enhancers**

**A3-12** (VUF 5455)



**A3-13**

**Fig. (7).** Allosteric enhancers for the adenosine receptor

in the control of motor behavior. Manipulation of A<sub>2A</sub>Rs might have therapeutic implications for neurodegenerative diseases such as Parkinson's disease. First, 3,7-dimethyl-1-propyl-xanthine was reported as an A<sub>2A</sub>R-selective antagonist, but it has low affinity and low A<sub>2A</sub>R-selectivity versus A<sub>1</sub>Rs [97]. Shimada *et al.* have successfully introduced the styryl group in the 8 position of xanthines to endow them with selective A<sub>2A</sub>R antagonistic properties [98,99]. On the other hand, starting from the non-selective adenosine antagonist CGS 15943 [100], a number of nonxanthine polyheterocycles have also been synthesized as A<sub>2A</sub>R antagonists. Development of A<sub>2A</sub>R ligands has been reviewed in several articles [41,101,102]. Tritiated CGS 21680 (Fig. 5, **A2A-2**) is a standard radioligand *in vitro* for A<sub>2A</sub>R assays [25,37-40]. Also [<sup>3</sup>H]KF17837 [103], [<sup>3</sup>H]SCH 58261 [25,104,105], [<sup>3</sup>H]ZM241385 [106,107] have high and A<sub>2A</sub>R-selective affinity and been used biochemical and pharmacological studies. So far KF17837 and several related xanthine analogs and a derivative of SCH 58261 have been evaluated as PET ligands (Fig. 8, Table 3), and only one xanthine-type ligand has been used in clinical studies by PET to date.

**4.1. PET Ligands**

First, a xanthine compound KF17837 developed by Suzuki and co-workers [98,99,103] was labeled with carbon-11 by *N*-methylation of the desmethyl compound using [<sup>11</sup>C]methyl iodide by two groups [108-110]. Stone-Elander *et al.* evaluated [<sup>11</sup>C]KF17837 by PET imaging of the monkey brain and concluded the limited usefulness as a ligand for mapping of A<sub>2A</sub>Rs because of low brain uptake and the apparently high nonspecific binding *in vivo* [109]. On the

other hand, Ishiwata and co-workers found that [<sup>11</sup>C]KF17837 was accumulated higher in the A<sub>2A</sub>R-rich striatum than in other brain regions (the uptake ratios to be up to 2.1) in mice, rats and monkeys. However, they suggested that due to the presence of high nonspecific binding as well as an unknown but specific binding of [<sup>11</sup>C]KF17837 in the other brain regions, the receptor-binding sites of xanthine-type ligands *in vivo* may be slightly different from those of nonxanthine-type A<sub>2A</sub> antagonists [110].

Then, Ishiwata *et al.* investigated the other xanthine-type radioligands, [<sup>11</sup>C]KF18446, [<sup>11</sup>C]KF19631 and [<sup>11</sup>C]CSC in rodents, and compared them with [<sup>11</sup>C]KF17837 [111]. [<sup>11</sup>C]KF19631 and [<sup>11</sup>C]CSC had similar properties as [<sup>11</sup>C]KF17837. However, [<sup>11</sup>C]KF18446 (later designated as [<sup>11</sup>C]TMSX) showed more preferable characteristics for mapping A<sub>2A</sub>Rs: a high incorporation into the brain and a high uptake ratio of striatum to the other regions (up to 3.2). PET imaging of the monkey brain showed high incorporation and a rapid clearance pattern, but the striatum was clearly visualized. [<sup>11</sup>C]CSC with less affinity for A<sub>2A</sub>Rs was also reported by Marian *et al.* [112]. [<sup>11</sup>C]KF18446 was further characterized *in vitro* and *in vivo* [113]. KF18446 had very low affinity *in vitro* for 13 neuroreceptors including adrenergic, dopamine and serotonin receptors. In a blocking study using various A<sub>2A</sub>R and A<sub>1</sub>R ligands *in vivo*, the cerebral cortex and cerebellum showed A<sub>2A</sub>R-specific uptake of [<sup>11</sup>C]KF18446 in a much lesser extent than the striatum. The K<sub>d</sub> values of [<sup>11</sup>C]KF18446 *in vitro* were 9.8 nM at the striatum and 16 nM at the cerebral cortex. These findings demonstrated that the binding sites of [<sup>11</sup>C]KF18446 were slightly different between striatum and other regions of the brain. Fredholm and co-workers also observed the

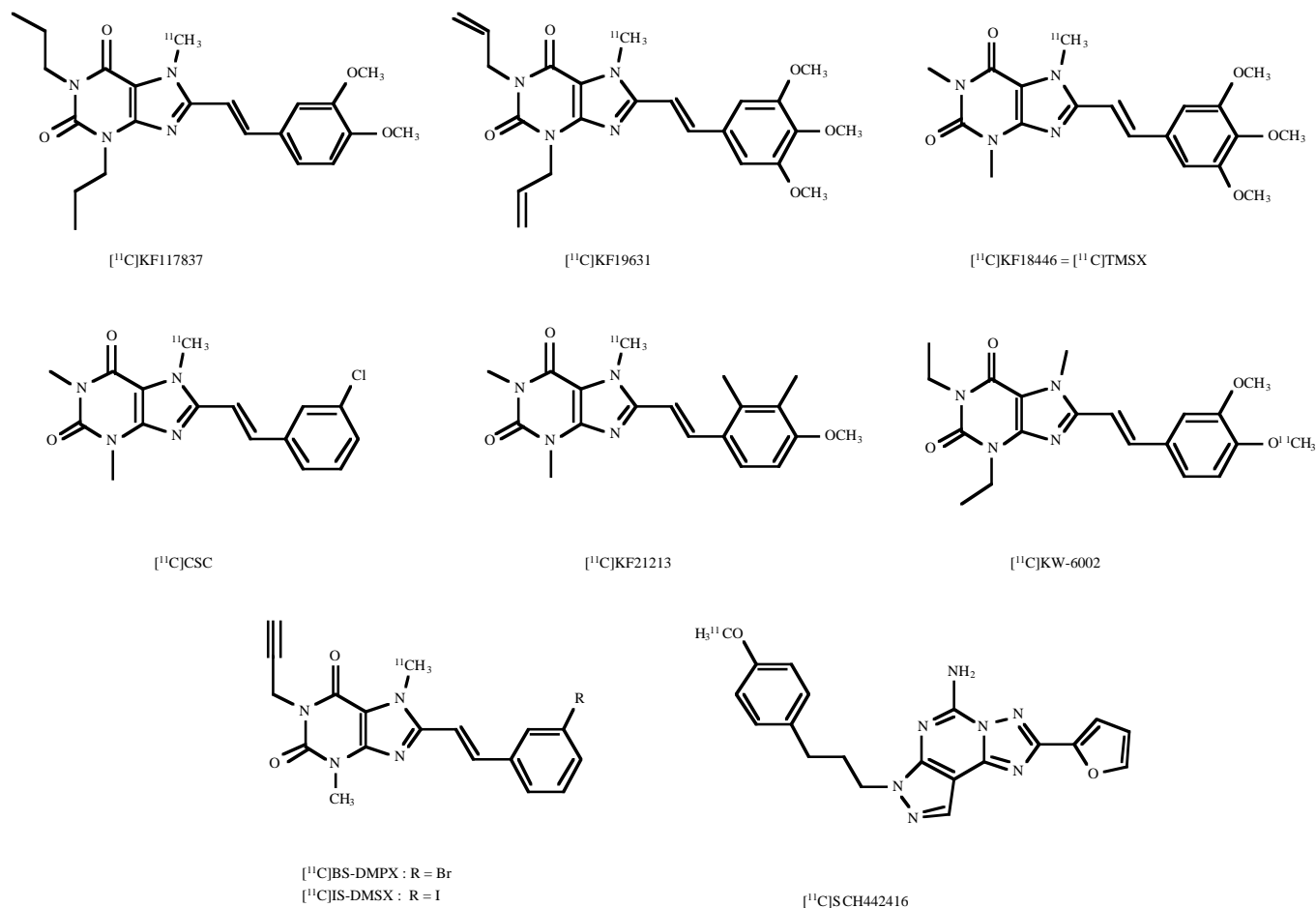


Fig. (8). PET ligands for adenosine A<sub>2A</sub> receptor

Table 3 Binding Affinities of Adenosine A<sub>2A</sub> Receptor Ligands

	Affinity (K <sub>i</sub> , nM)		Selectivity	Reference
	A <sub>1</sub>	A <sub>2A</sub>	A <sub>1</sub> /A <sub>2A</sub>	
KF17837	62	1.0	62	[94]
KF19631	860	3.5	250	[111]
KF18446 = TMSX	1600	5.9 K <sub>d</sub> , 9.8	270	[111] [113]
CSC	28000	54	520	[21]
BS-DMPX	2300	7.7	300	[119]
IS-DMPX	>10000	8.9	>1100	[119]
KF21213	>10000	3.0	>3300	[122]
KW-6002	150	2.2	68	[123]
SCH442416	1800 1100 (h)	0.50 0.048 (h)	3600 23000 (h)	[130]

binding sites of an A<sub>2A</sub>R radioligand in the cerebral cortex and hippocampus, and defined other A<sub>2A</sub>R subtypes, atypical A<sub>2A</sub>R, in contrast to the classical A<sub>2A</sub>R in the striatum [114,115]. In a rat model of degeneration of striatopallidal

gamma-aminobutyric acid-ergic-enkephalin neurons induced by intrastriatal injection of quinolinic acid, a Huntington's disease model, degeneration of A<sub>2A</sub>Rs in the lesioned striatum was detected by PET and *ex vivo* and *in vitro* autoradio-

graphy using [ $^{11}\text{C}$ ]KF18446 to a similar extent as degeneration of dopamine  $D_2$  receptors [116]. Furthermore, an *ex vivo* autoradiography study showed that [ $^{11}\text{C}$ ]KF18446, but not [ $^{11}\text{C}$ ]raclopride for dopamine  $D_2$  receptors, was incorporated into the globus pallidus to a lesser extent (the striatum-to-globus pallidus uptake ratio = approximately 0.6) and remarkably reduced uptake in the lesioned side [117]. The findings suggest that [ $^{11}\text{C}$ ]KF18446 is a candidate tracer for imaging the pallidal terminals projecting from the striatum. Thus, after preclinical studies including dosimetry and toxicology [118], [ $^{11}\text{C}$ ]KF18446 (designated as [ $^{11}\text{C}$ ]TMSX) was applied to clinical studies.

Ishiwata *et al.* further advanced seeking  $A_{2A}$ R-selective radioligands from two angles. First, they investigated the potential of brominated and iodinated styrylxanthine derivatives: [ $^{11}\text{C}$ ]BS-DMPX and [ $^{11}\text{C}$ ]IS-DMPX [119], based on BS-DMPX and its chlorinated analog CS-DMPX proposed by Müller *et al.* [120,121]. The former is potentially labeled with the positron emitter bromine-75 (half-life of 1.7 h) or bromine-76 (half-life of 16.1 h) and the latter with iodine-124 (half-life of 4.18 days) and iodine-123 (half-life of 13.3 h), resulting in the formation of PET and SPECT ligands, respectively. Both radioligands had high and selective affinity for  $A_{2A}$ Rs, but showed similar characteristics as observed for [ $^{11}\text{C}$ ]KF17837, [ $^{11}\text{C}$ ]KF19631 and [ $^{11}\text{C}$ ]CSC. The tracers accumulated slightly more in the striatum than in other regions of the brain, but the uptake ratios of striatum to other regions were low. In addition, the tracers not only exhibited specific binding to  $A_{2A}$ R in the target striatum, but also had specific binding to a certain extent and/or high nonspecific binding in the non-target tissues such as the cerebral cortex and cerebellum. Moreover, the search for radioligands with more pronounced  $A_{2A}$ R-selectivity, in other words much less affinity for non-target tissues, led to [ $^{11}\text{C}$ ]KF21213 [122]. In mice, the uptake ratio of striatum to cortex and striatum to cerebellum increased to 8.6 and 10.5, respectively, at 60 min postinjection, and the  $A_{2A}$ R-specific uptake was not detected in the cerebral cortex and cerebellum. In spite of these preferable properties of [ $^{11}\text{C}$ ]KF21213 in rodents, [ $^{11}\text{C}$ ]KF18446 ([ $^{11}\text{C}$ ]TMSX) exhibited a larger signal-to-noise ratio (difference uptake between striatum and cerebellum) than [ $^{11}\text{C}$ ]KF21213 in a preliminary PET study of the monkey brain, suggesting that [ $^{11}\text{C}$ ]TMSX is the most suitable tracer for mapping  $A_{2A}$ Rs by PET among the xanthine-type tracers proposed to date. Furthermore, a preliminary PET study in a monkey showed better brain kinetics for [ $^{11}\text{C}$ ]TMSX than for [ $^{11}\text{C}$ ]KF21213.<sup>1</sup>

The other xanthine-type radioligand [ $^{11}\text{C}$ ]KW-6002 was also investigated by Hirani *et al.* [123]. This tracer again showed similar characteristics as observed in [ $^{11}\text{C}$ ]KF17837, and had a limited potential for mapping  $A_{2A}$ Rs. Still [ $^{11}\text{C}$ ]KW-6002 may be applied in the development of the unlabeled compound as the antiparkinsonian agent [124,125], and KW-6002 (istradefylline) is currently undergoing clinical evaluation [126,127].

All of the xanthine-type radioligands described above were prepared by *N*- or *O*-methylation of the corresponding demethyl compounds using [ $^{11}\text{C}$ ]methyl iodide with high radiochemical yields suitable for routine clinical use. As the methylating agent, [ $^{11}\text{C}$ ]methyl triflate could be also used more efficiently as shown for the synthesis of [ $^{11}\text{C}$ ]TMSX [128]. On the other hand, it should be noted that a styryl group in xanthine derivatives is isomerized by exposure to visible light to form a stable equilibrium mixture of *E*-isomer and *Z*-isomer and the *Z*-isomer is less active than the *E*-isomer [129]. Therefore, in the experimental and clinical studies, all procedures from radiosynthesis to metabolites analysis of plasma samples of animals or humans for quantitative evaluation of ligand-receptor binding, should be carefully done under the exclusion of light [118].

As for the non-xanthine type radioligands, Todde *et al.* proposed [ $^{11}\text{C}$ ]SCH442416 derived from SCH 58261 [130]. In rats, the level of radioactivity in the striatum increased for the first 15 min after the injection of [ $^{11}\text{C}$ ]SCH442416 and, then gradually decreased. The maximal uptake ratios of striatum to cortex or to cerebellum were 4.6 at 15 min postinjection. Using various ligands, Moresco *et al.* [131] demonstrated in a blocking study in rats that the striatal uptake of [ $^{11}\text{C}$ ]SCH442416 is  $A_{2A}$ R-selective. Tracer uptake was significantly reduced following quinolinic acid-induced lesion as was found for [ $^{11}\text{C}$ ]TMSX [117]. In PET studies in monkeys, the binding potential values reflecting the binding of [ $^{11}\text{C}$ ]SCH442416 to  $A_{2A}$ Rs were 0.74, 0.16 and 0.13 in the striatum, cerebral cortex and cerebellum, respectively. These findings indicate that [ $^{11}\text{C}$ ]SCH442416 is a promising tracer for mapping  $A_{2A}$ Rs. Regarding the uptake ratio of striatum to reference tissues in the rat brain and the brain kinetics in the monkey brain, [ $^{11}\text{C}$ ]SCH442416 may be a better tracer than [ $^{11}\text{C}$ ]TMSX.

## 4.2. Clinical Studies

The first visualization of  $A_{2A}$ Rs in the human brain was reported by Ishiwata and co-workers using [ $^{11}\text{C}$ ]TMSX PET, and was compared with dopamine  $D_2$  receptors ([ $^{11}\text{C}$ ]raclopride PET) and  $A_1$ Rs ([ $^{11}\text{C}$ ]MPDX PET) [132]. They demonstrated that infusion of theophylline reduced the [ $^{11}\text{C}$ ]TMSX-binding evaluated Dv.

The group preliminary applied [ $^{11}\text{C}$ ]TMSX PET to Parkinson's disease. Fig. (9) demonstrates the change of  $A_{2A}$ Rs in patients with early Parkinson's disease measured by [ $^{11}\text{C}$ ]TMSX<sup>2</sup>. Three characteristics of neurosynaptic situations are shown: the dopamine transporter with [ $^{11}\text{C}$ ]CFT, the dopamine  $D_2$  receptor with [ $^{11}\text{C}$ ]raclopride, and the  $A_{2A}$ R with [ $^{11}\text{C}$ ]TMSX. The  $B_p$  was computed using EPICA [87] with the central semiovale as a reference region [133].

In early Parkinson's disease, release of dopamine is asymmetrically affected. In the patient in this study, the symptoms of Parkinson's disease were right dominant. The left-side dopamine transporter was more decreased than the

<sup>1</sup> Ishiwata, K.; Tsukada, H.; Kimura, Y.; Kawamura, K.; Harada, N.; Hendrikse, N.H. In vivo evaluation of [ $^{11}\text{C}$ ]TMSX and [ $^{11}\text{C}$ ]KF21213 for mapping adenosine  $A_{2A}$  receptors: brain kinetics in the conscious monkey and P-glycoprotein modulation in the mouse brain. 22nd International Symposium Cerebral Blood Flow, Metabolism, and Function & 7th International Conference of Quantification of Brain Function with PET, 2005, BP-76, Amsterdam.

<sup>2</sup> Mishina, M.; Ishii, K.; Kitamura, S.; Kimura, Y.; Naganawa, M.; Hashimoto, M.; Suzuki, M.; Oda, K.; Hamamoto, M.; Kobayashi, S.; Katayama, Y.; Ishiwata, K. Distribution of adenosine  $A_{2A}$  receptors in de novo Parkinson's disease using  $^{11}\text{C}$ -TMSX PET — a preliminary study, Targeting adenosine  $A_{2A}$  receptors in Parkinson's disease and other CNS, P-44, Boston, MA, 2006.

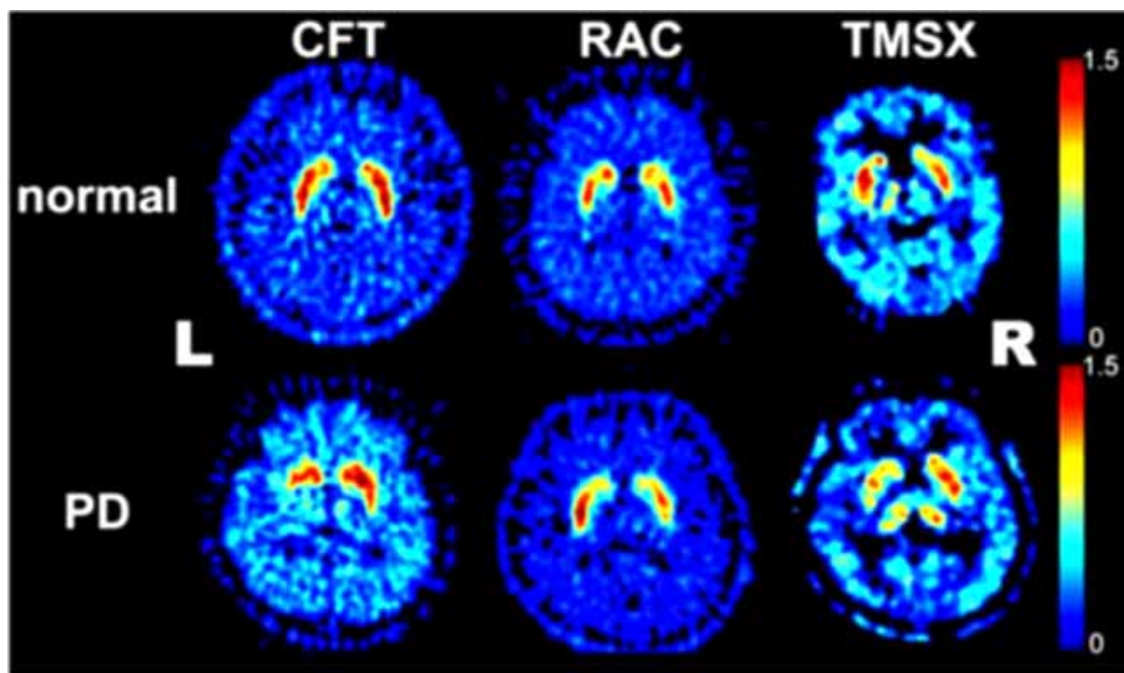


**Fig. (9).** PET Images of adenosine  $A_{2A}$  receptor using [ $^{11}\text{C}$ ]TMSX in Parkinson's disease. The upper and lower rows represent a normal subject and a patient with Parkinson's disease, respectively. The [ $^{11}\text{C}$ ]CFT and [ $^{11}\text{C}$ ]raclopride images are static images, while the [ $^{11}\text{C}$ ]TMSX images represent binding potentials which are related to a density of receptor binding sites.

right-side one, and the  $D_2$  receptors bindings was increased bilaterally. The  $A_{2A}R$  was decreased on the left side. These observation imposes that the changes in  $A_{2A}R$  binding measured with [ $^{11}\text{C}$ ]TMSX are coupled with the asymmetry of the symptoms. The pathophysiological interpretation still has to be investigated in future work. Since a reciprocal relationship between dopamine  $D_2$  receptors and  $A_{2A}R$ s was reported previously [134],  $A_{2A}R$ s imaging with [ $^{11}\text{C}$ ]TMSX warrants further investigation.

### 4.3. Medicinal Chemistry

#### 4.3.1. $A_{2A}$ Agonists

Promising candidate agonists for PET-labeling have not been described in the literature thus far. Potent  $A_{2A}R$  subtype selective compounds have been reported but none of these are amenable for labeling with carbon-11 or fluorine-18. An example is YT-146 (**A2A-1**, Fig. 5), an octynyl derivative of adenosine, which has an appropriate logP value and a fairly good selectivity of  $A_{2A}$  over  $A_1$ . An  $A_{2A}R$  subtype selective agonist that can be labeled in the ethyl group is the established compound CGS 21680 (**A2A-2**). This compound is used as a standard for  $A_{2A}R$  in *in vitro* studies, but the low log P value will make the PET-labeled form of CGS 21680 not suitable for investigating cerebral adenosine receptors.

#### 4.3.2. $A_{2A}$ Antagonists

Antagonists for this receptor subtype can be divided in two main categories, i.e. xanthine-type and polyheterocyclic compounds.  $A_{2A}R$  antagonists are orally effective in a variety of rodent models of Parkinson's disease [13]. Extensive

optimization among the xanthine derivatives has already led to the clinical candidate KW-6002 (Fig. 8) (Kyowa Hakkō Kogyō Co Ltd) [124-127], which was labeled with carbon-11 (see section 4.1). However, there is an increasing interest among researchers in this field to explore other classes of compounds as potential antagonists for this particular receptor.

From both classes of compounds potent and selective candidates have emerged that are amenable for labelling with carbon-11 or fluorine-18 (Fig. 10). These compounds have high affinity, selectivity and a suitable lipophilicity to penetrate the blood brain barrier. The selectivity is based on  $A_1$  and  $A_{2A}$  affinities, and no affinities for  $A_{2B}$  or  $A_3$  have been determined. As described above, most obvious labeling possibilities are [ $^{11}\text{C}$ ]methylation of one of the aromatic methoxy groups or the *N*-methyl in the xanthine part. The  $^{11}\text{C}$ -labeling procedure for this *N*-methyl group has been developed for other xanthines previously and can be applied to candidate **A2A-3** [173].

Several potent candidates from the polyheterocyclic class have also been proposed. These compounds have excellent  $A_{2A}$  over  $A_1$  selectivity and logP values ranging from 0.6 to 3.3. These compounds can be labeled with carbon-11 or fluorine-18, but as illustrated for compounds (**A2A-7**, **-8** and **-12**) evaluated by Holschbach *et al.* [135,136], these properties are no guarantee to become a useful PET-tracer. In particular the compounds as described by Minetti *et al.* (**A2A-4**, **-5** and **-6**) [137], Peng *et al.* (**A2A-9**, **-10** and **-11**) [138], Vu *et al.* (**A2A-13**, **-14** and **-15**) [139,140] and by Matasi *et al.* (**A2A-16** and **-17**) [141,142] are candidates for PET-labeling.

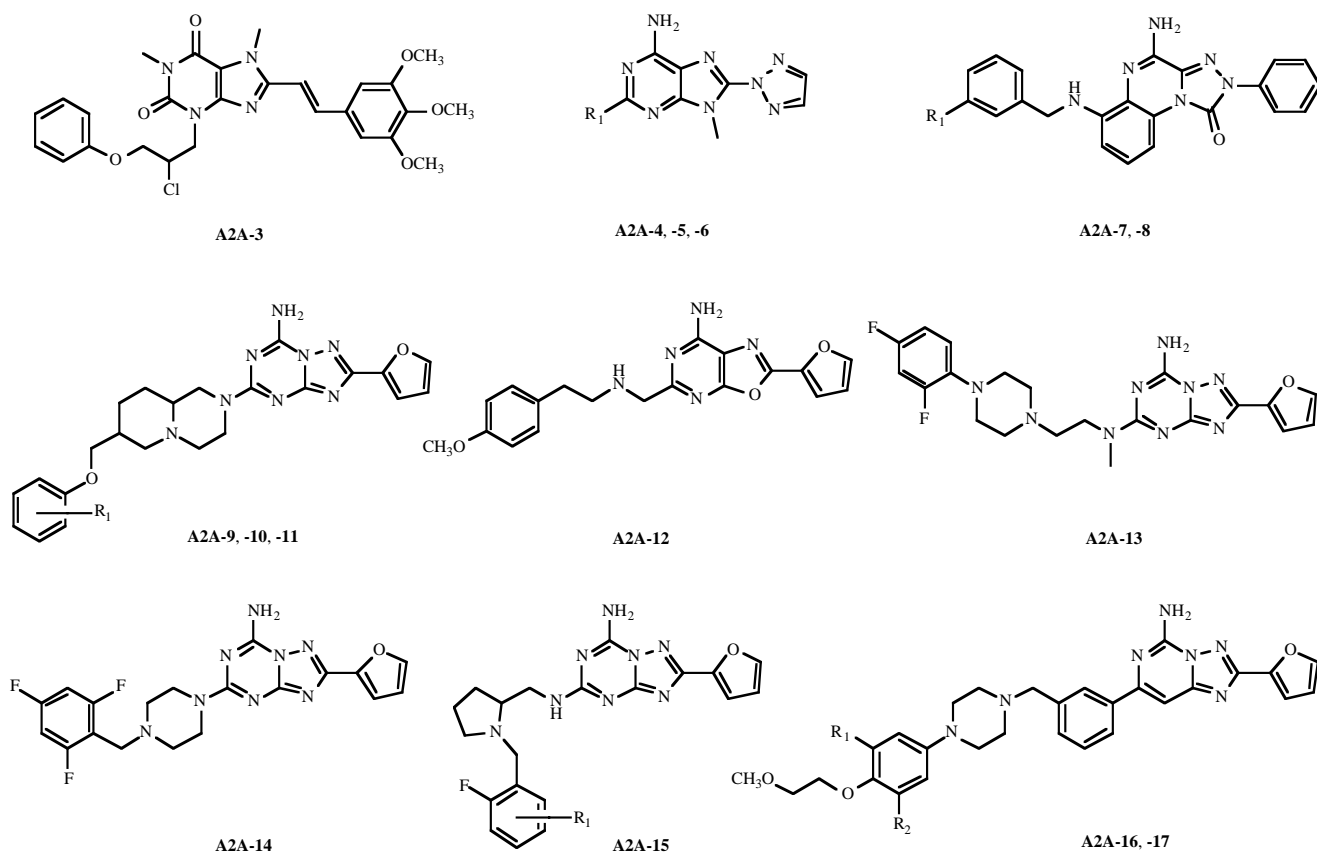


Fig. (10). Adenosine A<sub>2A</sub> receptor antagonists

## 5. ADENOSINE A<sub>2B</sub> RECEPTOR

### 5.1. Introduction

While the A<sub>1</sub>R, A<sub>2A</sub>R and A<sub>3</sub>R have been pharmacologically characterized through the use of highly potent and selective agonists and/or antagonists, the study of the A<sub>2B</sub>R subtype has been precluded due to the lack of selective ligands, and the absence of an appropriate binding assay. To date, the most potent, but nonselective, agonist for this subtype is NECA (Table 2), with affinity in the micromolar range [4]. No PET tracer for this subtype has been described so far.

The A<sub>2B</sub>R has been implied in vascularization, cell proliferation, differentiation and in mast-cell-mediated activation of angiogenesis. This last effect is the result of a cooperative action of the A<sub>2</sub>Rs [143]. Peripherally, activation of the receptor leads to release of inflammatory cytokines. Antagonists are believed to be useful in the treatment of asthma.

It has not been demonstrated whether A<sub>2B</sub>Rs are present in the brain or what their function would be. For the sake of completeness and anticipating to possible future applications for the A<sub>2B</sub>R subtype for neuroscience, some potential compounds will be described in section 5.2.

### 5.2. Medicinal Chemistry

Regarding suitable agonists, no compound has been reported that has high affinity, selectivity or an acceptable lipophilicity and is amenable for labeling with carbon-11 or fluorine-18.

With respect to antagonists, several candidates draw attention (Table 4, Fig. 11). Except for OSIP-339391 (A2B-6) [174], all compounds belong to the class of xanthines. A2B-1 has very high affinity for the A<sub>2B</sub>R, but for the other adenosine receptor subtypes, affinities are very low [175]. The xanthine moiety contains 2 *N*-methyl groups. One of these could be replaced by an [<sup>11</sup>C]methyl group. Replacement of the CF<sub>3</sub>-group in A2B-1 by a fluorine atom decreases the affinity and selectivity for the A<sub>2B</sub>R but may still yield a suitable PET-tracer that may be labeled with fluorine-18 (A2B-2) [176].

Ilas *et al.* reported potent A<sub>2B</sub>R ligands for electron paramagnetic resonance [144]. Ji *et al.* developed quite analogous compounds by replacing the radical part in A2B-3 by a cyanophenyl group (A2B-5) [145]. This compound displayed even higher affinity for the A<sub>2B</sub>R and retained its selectivity, but has a high logP possibly resulting in high non-specific binding. A2B-4 as reported by Baraldi *et al.* offers labeling possibilities by *N*-methylation with [<sup>11</sup>C]methyl iodide or [<sup>11</sup>C]methyl triflate on the pyrazole ring [146]. An alternative approach could be [<sup>11</sup>C]propylation on the amidic nitrogens in the xanthine ring. Finally, OSIP-339391 has the highest affinity and a good selectivity for the A<sub>2B</sub>R. PET-labeling may be possible by [<sup>11</sup>C]acetylation.

## 6. ADENOSINE A<sub>3</sub> RECEPTOR

### 6.1. Introduction

Among the human adenosine receptor subtypes, the A<sub>3</sub>R subtype was most recently characterized [7,8,147]. The A<sub>3</sub>R is a 318 amino acid protein that exhibits only 72% and

Table 4. Affinities and Subtype Selectivities of a Selection of Adenosine Receptor Antagonists

Compound	Substituents			$K_i$ (nM)					
	R <sub>1</sub>	R <sub>2</sub>	X	LogP <sup>a</sup>	hA <sub>1</sub>	hA <sub>2a</sub>	hA <sub>2b</sub>	hA <sub>3</sub>	Ref.
<i>A<sub>1</sub> selective</i>									
DPCPX				3.4	3.0	60		243	[52]
A1-2				5.7	25			1540	[52]
A1-3 (LUF 5735)				4.4	3.7				[92]
A1-4 (LUF 5608)				2.9	7.7			14200	[95]
<i>A<sub>2A</sub> selective</i>									
A2A-3				3.0	>10000	44			[173]
A2A-4	H			-0.5	0.4	46.3			[137]
A2A-5	Pentyl			1.8	26.2	3.3			[137]
A2A-6	EtPh			1.8	80	4.7			[137]
A2A-7	p-OMe			1.7	22	24			[135]
A2A-8	p-F			1.8	22	29			[135]
A2A-9	m-F			1.6	3300	0.2			[138]
A2A-10	o-F			1.6	>500	0.9			[138]
A2A-11	p-F			1.6	>500	4			[138]
A2A-12				1.1	1570	22			[136]
A2A-13				1.5	750	6.5			[139,140]
A2A-14				0.6	1300	3			[139,140]
A2A-15	F-isomers			1.1	>250	2.8			[139,140]
A2A-16	MeO	H		3.3	442	3.3			[141]
A2A-17	F	F		3.2	744	2.2			[142]
<i>A<sub>2B</sub> selective</i>									
A2B-1	CF <sub>3</sub>			Unknown	990	690	1	1000	[175]
A2B-2	F			Unknown	460	200	27		[175]
A2B-3				Unknown	15	1270	48	350	[144]
A2B-4				3.0	248	>1000	1.7	>1000	[146]
A2B-5				5.0	>50	>50	1.2	>50	[145]
A2B-6 (OSIP-339391)				1.4	37	328	0.5	450	[174]
<i>A<sub>3</sub> selective</i>									
A3-3a	Et	4-MeOPh		2.1	1026	1045		0.28	[146]
A3-3b	nPr	4-MeOPh		2.7	1197	141		0.29	[146]
A3-3c	Me	4-pyridinyl.HCl		Unknown	355	110	>1000	0.014	[154]
A3-4a	F			3.2		510		0.25	[155]



## 6.2. Medicinal Chemistry

### 6.2.1. A<sub>3</sub> Agonists

The majority of selective A<sub>3</sub>R agonists are N<sup>6</sup> and/or C2 substituted adenosine derivatives with an N-methylamide substituent at the 5' position. In theory, a carbon-11 label can be introduced in these compounds by N-methylation. The m-iodobenzyl derivative IB-MECA (**A3-1a**) is an important lead compound for A<sub>3</sub>R agonists (Table 2, Fig. 5. IB-MECA is in phase II clinical trials for the treatment of colorectal cancer and rheumatoid arthritis now, but it is only moderately selective for the A<sub>3</sub>R subtype and therefore not an ideal candidate for a PET tracer. The A<sub>1</sub>/A<sub>3</sub> selectivity was increased by substitution of a chlorine atom at C2, as in Cl-IB-MECA (**A3-1b**), although the affinity for the A<sub>3</sub>R was slightly reduced [151]. When the oxygen atom in the ribose ring is additionally replaced by sulfur, as in **A3-1c**, the affinity and selectivity is further increased [152]. Besides labeling with carbon-11, the m-iodobenzyl substituent also allows labeling of compounds **A3-1a**, **-1b** and **-1c** with iodine isotopes for SPECT imaging or with the long-lived PET isotope iodine-124 (half-life of 4.18 days). The most potent and A<sub>3</sub>-selective thioadenosine derivative that was reported by Jeong and coworkers, was the N<sup>6</sup>-methyl compound LJ530 (**A3-1d**) [152], which can be labeled with carbon-11 either at the 5'-amide or at N<sup>6</sup>. Unfortunately, this compound appears too hydrophilic (logP 0.5) for brain penetration.

A<sub>3</sub>R binding is favored when the ribose ring is in the 2'-exo-(N) twist conformation. As an approach to increase A<sub>3</sub>-selectivity by increasing the rigidity of the ribose moiety, Tchilibon *et al.* prepared a series of 2,N<sup>6</sup>-disubstituted (N)-methanocarba adenosine derivatives [153]. Compounds **A3-2a**, **-2b** and **-2c** are some representatives from this study with a high affinity and selectivity for the A<sub>3</sub>R. These compounds are readily labeled by [<sup>11</sup>C]methylation at the methoxy group. In addition, compound **A3-2c** can also be labeled with various iodine isotopes for SPECT or PET. Based on the lipophilicity of these compounds, iodide **A3-2c** seems to be the most likely candidate as a PET tracer for imaging the CNS A<sub>3</sub>R.

### 6.2.2. A<sub>3</sub> Antagonists

In contrast to the strict structural limitations of A<sub>3</sub>R agonists, highly potent antagonists of this receptor subtype from various distinct classes of compounds have been described. Baraldi and coworkers prepared several pyrazolo[4,3,-e]-1,2,4-triazolo[1,5-c]pyrimidine derivatives [146]. From these compounds, **A3-3a** and **-3b** were depicted in Fig. (12) and Table 4, as highly potent representatives with high selectivity for the A<sub>3</sub>R. Both substances can be labeled with carbon-11 and have favorable lipophilicity for crossing the blood-brain-barrier. To increase the water solubility of these compounds, positively charged pyridine substituents were attached to the carbamate moiety, resulting in e.g. compound **A3-3c** [154]. This compound had an exceptionally high affinity and selectivity for the A<sub>3</sub>R, but it is unclear whether this charged compound could penetrate the brain. The free base of **A3-3c** had similar affinity and selectivity as the hydrochloride salt and a logP of 1.1. The closely related compounds **A3-4a**, **-4b** and **-4c** are representatives of the 1,2,4-triazole[5,1-i]purine class of A<sub>3</sub>R antagonist that were pub-

lished by Okamura *et al.* [155]. These antagonists have subnanomolar affinity and excellent selectivity for the A<sub>3</sub>R subtype. Purines **A3-4b** and **-4c** are amenable for [<sup>11</sup>C]methylation, whereas **A3-4a** can be labeled by nucleophilic substitution with [<sup>18</sup>F]fluoride. The imidazopyridinone derivative PSB-11 (**A3-5**) was described by Müller *et al.* as a high affinity, selective A<sub>3</sub> antagonist that is approximately 4 times more potent than its S-enantiomer [156]. PSB-11 was radiolabeled with tritium and applied in binding assays [157]. Remarkably, non-specific binding of [<sup>3</sup>H]PSB-11 in these assays was extraordinary low (approximately 2%). PSB-11 might therefore be an attractive candidate PET tracer, as it can readily be labeled by N-[<sup>11</sup>C]methylation.

The structurally closely related pyrazolo[3,4-c]quinoline **A3-6** [158] and 1,2,4-triazolo[4,3-a]quinoxaline **A3-7** [159], the isoquinoline VUF5574 (**A3-8**) [160], the thiazole **A3-9a** and the thiadiazole **A3-9b** [161] have a methoxy substituent that can be exploited for labeling with carbon-11. All these compounds have an affinity for the A<sub>3</sub>R in the low nanomolar range and all are highly selective antagonist for this receptor subtype. Compounds **A3-6**, **-8**, **-9a** and **-9b** seem to have a favorable lipophilicity for brain imaging, whereas the logP of **A3-7** may be to low for brain penetration.

Finally, Li and coworkers reported various substituted pyridine derivatives as selective A<sub>3</sub> antagonists, such as fluoride **A3-10** [162] and methoxy compound **A3-11** [163]. These pyridine derivatives, however, are not likely candidates for PET tracers, because of their high lipophilicity.

### 6.2.3. A<sub>3</sub> Allosteric Enhancers

Isoquinoline derivative VUF5455 (**A3-12**) was among the first allosteric enhancers of the A<sub>3</sub>R to be discovered [164] and can readily be labeled by [<sup>11</sup>C]methylation at the methoxy group (Fig. 7). VUF5455 significantly reduced the dissociation rate of an A<sub>3</sub> agonist, but did not affect the dissociation of an A<sub>3</sub> antagonist. VUF5455 did not show any binding to the A<sub>1</sub>R and A<sub>2A</sub>R, but it had a weak affinity for the binding site of the A<sub>3</sub>R.

Quinoline derivative DU124,183 has been used as a lead compound for allosteric enhancers of the A<sub>3</sub>R, but it can not easily be labeled with carbon-11. Compound **A3-13** is the methoxy-substituted analogue of DU124,183, in which a [<sup>11</sup>C]methyl group can be introduced at the methoxy substituent. Compound **A3-13** exhibits similar allosteric enhancement activity as DU124, 183 and hardly displays any affinity for the binding sites of the different adenosine receptor subtypes [165].

A potential drawback for application of radiolabeled VUF5455 or **A3-13** as a PET tracer could be their relatively high lipophilicity (logP 3.6 and 3.7, respectively).

## 7. ADENOSINE UPTAKE SITE

### 7.1. Introduction

Hydrophilic nucleosides, including adenosine, rely on carrier proteins for their transport across membranes [166]. Two families of transporters have been identified, the equilibrative and concentrative nucleoside transporters (ENT and CNT, respectively). Although nucleoside salvage is the main

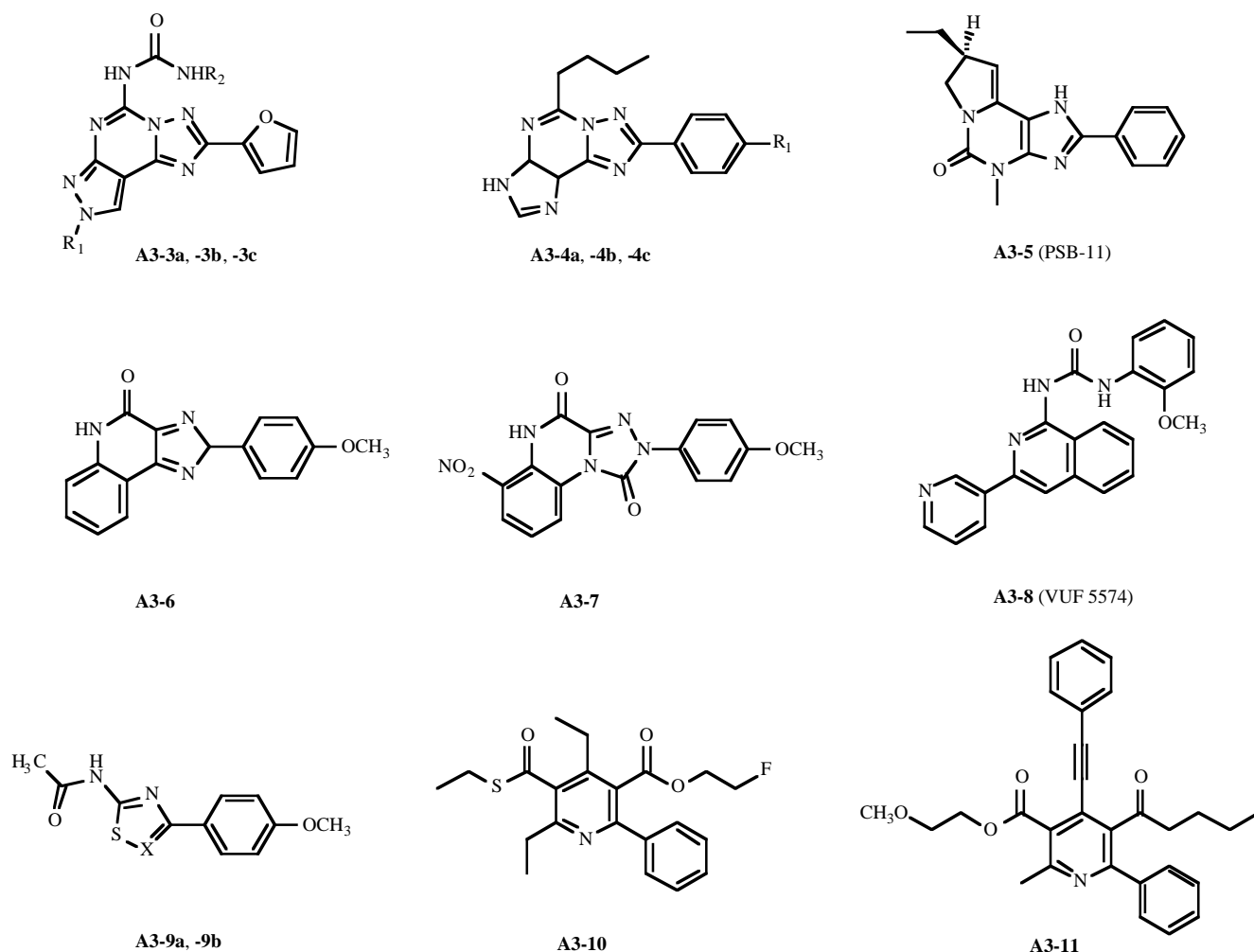


Fig. (12). Adenosine A<sub>3</sub> receptor antagonists

function of the transporter, recent data indicate functions beyond metabolic recycling. In the brain and spinal cord, for example, the transporters regulate synaptic levels of neuroactive purines, such as adenosine, and thus have effect on physiological processes modulated through G-coupled adenosine receptors. Novel identified functions of the transporters within CNS are related to sleep, arousal, addiction, nociception and analgesia.

Regarding ENTs, two subtypes have been characterized, the es (equilibrative sensitive), also known as ENT1 and the ei (equilibrative insensitive) transporter, ENT2 [166]. These differences are based on the (in)sensitivity to inhibition by *S*<sup>6</sup>-(4-nitrobenzyl)-mercaptapurine riboside (**AUS-1a**, also called 4-nitrobenzylthioinosine, NBTI), and dipyridamole (**AUS-2**), a non-nucleoside, that inhibits both ENT1 and ENT2 (Fig. 13). Both NBTI and dipyridamole inhibit ENT1 at low nanomolar concentrations. Recently, two new subtypes, ENT3 and ENT4 were identified, but not yet characterized. ENTs are distributed all over the mammalian tissues, whereas the CNTs are especially abundant in the intestine, kidney, and liver. The CNT proteins can be divided in 3 subtypes, CNT1, CNT2, and CNT3. CNTs are insensitive towards inhibition by NBTI.

## 7.2. PET ligands

For PET-imaging only two papers appeared. [1-methyl-<sup>11</sup>C]-3-[1-(6,7-dimethoxyquinazolin-4-yl)piperidin-4-yl]-1,6-dimethyl-2,4(1*H*,3*H*)-quinazolin-2(1*H*)-one (<sup>11</sup>C]KF21652) with a K<sub>i</sub> value of 13 nM was prepared by *N*-[<sup>11</sup>C] methylation (Fig. 14) [167]. In biodistribution studies, the highest uptake was found in the liver, followed by the kidney and small intestine, and carrier-saturable uptake was observed only in the liver (about 30%). Although the brain uptake was very low *in vivo* probably because of relatively high lipophilicity (logP 3.6), *in vitro* autoradiography showed binding of [<sup>11</sup>C]KF21652 to adenosine transporters with a high fraction of nonspecific binding (specific binding, less than 25% of total binding).

The other labeled tracer is [<sup>11</sup>C]adenosine monophosphate ([<sup>11</sup>C]AMP) [168]. Extracellular adenylates undergo rapid conversion: ATP → ADP → AMP → adenosine, followed by cellular uptake and intracellular rephosphorylation to ATP. Adenylate imaging of cancer would be possible because of increased import/export of radiolabeled adenylates associated with tumor metabolism as well as adenylate interactions with adenosine receptors. [<sup>11</sup>C]AMP was produced by reacting [<sup>11</sup>C]formaldehyde with the corresponding

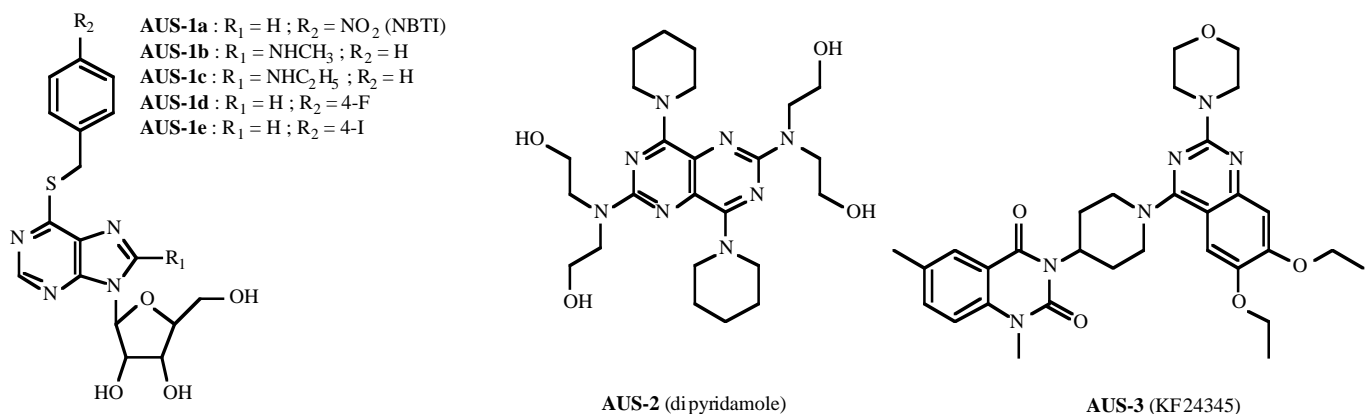


**Fig. (13).** Adenosine uptake site inhibitors

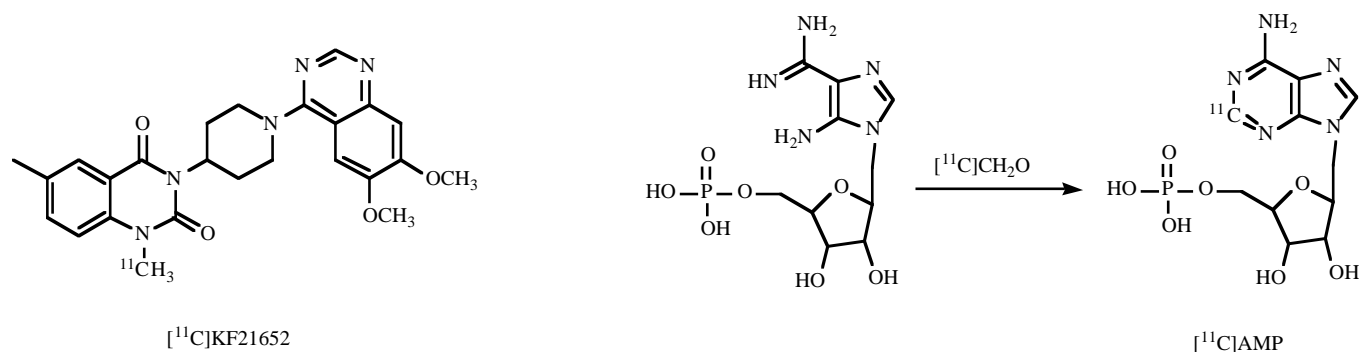


**Fig. (14).** PET ligands for the adenosine uptake site.

amino-imidazolyl-carboxamide (Fig. 14). Besides biodistribution studies, the effect on [<sup>11</sup>C]AMP uptake by blocking with dipyridamole was investigated. At 60 min postinjection lung uptake was reduced to about 40%. Uptake of [<sup>11</sup>C]AMP was highest in the lung, blood and heart. The value of this radioligand need to be further investigated.

### 7.3. Medicinal Chemistry

KF24345 (**AUS-3**) was developed as a novel anti-inflammatory agent and binds to both ENT1 and ENT2 (Fig. 13) [169]. As NBTI (K<sub>i</sub> of 0.7 nM) the K<sub>i</sub> for ENT1 was 0.4 nM, but KF24345 was 50-fold more effective at blocking ENT2 (K<sub>i</sub> of 100 nM). KF24345 is an interesting candidate for PET-labeling. [<sup>11</sup>C]Methylation on the amidic nitrogen is a potential labeling strategy.

A related series of analogs was developed with alkylamino substituents at the purine ring [170], aiming to prepare less polar compounds than NBTI (logP 1.20). This polar nature hinders its oral availability and passage through the blood brain barrier. It was shown that the addition of this alkylamino group had the concomitant advantage that affinity was greatly increased. K<sub>i</sub> values were in the nanomolar range, whereas without alkylamino these values were 53 nM. From the point of view of development of a PET-ligand, the NHMe compound is to be preferred, but increasing the alkyl group to ethyl or propyl further increases lipophilicity and affinity. In fact, introduction of the NH-methyl and NH-ethyl groups results in more polar compounds (**AUS-1b** and **AUS-**

**1c**, K<sub>i</sub> values of 28 nM and 9.5 nM, respectively) (logP 0.64 and 1.17, respectively). Larger alkyl groups, such as cyclohexyl, result in even more potent and lipophilic substances.

Another modification to increase effectiveness has been investigated by Gupte *et al.* [171]. Starting from NBTI as a lead compound, the nitro group was replaced by halogens in ortho, meta and para position. All the para-compounds with Br, Cl, I and F yielded the most potent inhibitors with K<sub>i</sub> values in the nanomolar range. The 4-fluoro compound (**AUS-1d**), a candidate for <sup>18</sup>F-labeling with a logP of 1.52, has a K<sub>i</sub> of 9.02 nM. Alternatively, <sup>124</sup>I-labeling would yield a compound (**AUS-1e**) with a K<sub>i</sub> of 3.88 nM.

### CONCLUSION

Development of high-affinity and subtype-selective ligands for adenosine receptors for last two decades has enabled quantitative measurement of A<sub>1</sub>R<sub>s</sub> of the human brain by PET using [<sup>18</sup>F]CPFPX or [<sup>11</sup>C]MPDX as an *in vivo* probe. The PET using these two tracers could be applied to evaluate the pathophysiological states of the receptors in humans with neurological and psychiatric disorders. Preliminary data on mapping of A<sub>2A</sub>R<sub>s</sub> in the human brain were generated using [<sup>11</sup>C]TMSX, but more studies are essential for establishing the method. On the other hand, in spite of increasing evidence characterizing pathophysiological events in the other subtypes, A<sub>2B</sub>R and A<sub>3</sub>R, and adenosine uptake site, their function has not clearly understood yet, and there were only limited trials for developing PET ligands for these

binding sites to date. However, continued efforts for seeking high-affinity and selective ligands in medicinal chemistry will lead PET probes suitable for these binding sites near future.

#### ABBREVIATIONS

CNS	= Central nervous system	ZM 241385	= triazolo[1,5-c]pyrimidine 4-(2-[7-amino-2-(2-furyl){1,2,4}triazolo{2,3-a}{1,3,5}triazin-5-yl-amino]ethyl)phenol
A <sub>1</sub> R	= Adenosine A <sub>1</sub> receptor	KF18446	= ( <i>E</i> )-8-(3,4,5-trimethoxystyryl)-1,3,7-trimethylxanthine
A <sub>2A</sub> R	= Adenosine A <sub>2A</sub> receptor	KF19631	= ( <i>E</i> )-1,3-diallyl-7-methyl-8-(3,4,5-trimethoxystyryl)xanthine
A <sub>2B</sub> R	= Adenosine A <sub>2B</sub> receptor	CSC	= ( <i>E</i> )-8-(3-chlorostyryl)-1,3,7-trimethylxanthine
A <sub>3</sub> R	= Adenosine A <sub>3</sub> receptor	BS-DMPX	= ( <i>E</i> )-8-(3-bromostyryl)-3,7-dimethyl-1-propargylxanthine
PET	= Positron emission tomography	IS-DMPX	= ( <i>E</i> )-3,7-dimethyl-8-(3-iodostyryl)-1-propargylxanthine
SPECT	= Single photon emission computed tomography	CS-DMPX	= ( <i>E</i> )-8-(3-chlorostyryl)-3,7-dimethyl-1-propargylxanthine
DPCPX	= 8-Cyclopentyl-1,3-dipropylxanthine	SCH442416	= 5-Amino-7-(3-(4-methoxyphenyl)propyl)-2-(2-furyl)pyrazolo[4,3-e]-1,2,4-triazolo[1,5-c]pyrimidine
KF15372	= 8-Dicyclopropylmethyl-1,3-dipropylxanthine	CFT	= 2 $\beta$ -Carbomethoxy-3 $\beta$ -(4-fluorophenyl) tropane
MPDX	= 8-Dicyclopropylmethyl-1-methyl-3-propylxanthine	OSIP-339391	= <i>N</i> -(2-{2-phenyl-6-[4-(2,2,3,3-tetratritio-3-phenylpropyl)-piperazine-1-carbonyl]-7H-pyrrolo[2,3-d]pyrimidin-4-ylamino}-ethyl)-acetamide
EPDX	= 8-Dicyclopropylmethyl-1-ethyl-3-propylxanthine	IB-MECA	= <i>N</i> <sup>6</sup> -(3-Iodobenyl)adenosine-5'- <i>N</i> -methyluronamide
CPFPX	= 8-Cyclopentyl-3-(3-fluoropropyl)-1-propylxanthine	Cl-IB-MECA	= 2-Chloro- <i>N</i> <sup>6</sup> -(3-iodobenyl)adenosine-5'- <i>N</i> -methyluronamide
FR194921	= 2-(1-Methyl-4-piperidinyl)-6-(2-phenylpyrazolo[1,5- <i>a</i> ]pyridin-3-yl)-3(2 <i>H</i> )-pyridazinone	LJ530	= 1-[2-Chloro-6-(methylamino)-9H-purin-9-yl]-1-deoxy- <i>N</i> -methyl-4-thio- $\beta$ -D-ribofuranuronamide
<i>B<sub>p</sub></i>	= Binding potential	PSB-11 (A3-5)	= (8 <i>R</i> )-8-Ethyl-1,4,7,8-tetrahydro-4-methyl-2-phenyl-5H-imidazo[2,1- <i>i</i> ]purin-5-one
<i>D<sub>v</sub></i>	= Distribution volume	VUF5574 (A3-8)	= <i>N</i> -(2-Methoxyphenyl)- <i>N</i> -[2-(3-pyridyl)quinazolin-4-yl]urea
NECA (A1-1a)	= Adenosine-5'-ethyluronamide ( <i>N</i> -ethylcarboxamidoadenosine)	VUF5455	= 4-Methoxy- <i>N</i> -[7-methyl-3-(2-pyridinyl)-1-isoquinolinyl]benzamide
CPA (A1-1c)	= <i>N</i> <sup>6</sup> -Cyclopentyladenosine	DU124,183	= 2-Cyclopentyl-4-phenylamino-1H-imidazo[4,5- <i>c</i> ]quinoline
CCPA (A1-1d)	= 2-Chloro- <i>N</i> <sup>6</sup> -cyclopentyladenosine	ENT	= Equilibrative nucleoside transporter
CPA (A1-1e)	= <i>R</i> -PIA; <i>R</i> - <i>N</i> <sup>6</sup> -(phenylisopropyl)-adenosine	CNT	= Concentrative nucleoside transporter
LUF5735 (A1-3)	= <i>N</i> -(4,6-diphenyl-2-pyrimidinyl)-butanamide	NBTI	= <i>S</i> <sup>6</sup> -(4-Nitrobenzyl)-mercaptapurine riboside (4-nitrobenzylthioinosine)
LUF5608 (A1-4)	= <i>N</i> <sup>6</sup> -cyclopentyl-8-( <i>N</i> -methylisopropylamino)-9-methyladenine	KF21652	= 3-[1-(6,7-Dimethoxyquinazolin-4-yl)piperidin-4-yl]-1,6-dimethyl-2,4(1 <i>H</i> , 3 <i>H</i> )-quinazolin-2-one
PD 81,723	= (2-Amino-4,5-dimethyl-3-thienyl)-[3-(trifluoromethyl)-phenyl]-methanone		
CGS 15943	= 5-Amino-9-chloro-2-(2-furyl)-[1,2,4]-triazolo[1,5- <i>c</i> ]quinazoline		
CGS 21680	= 2- <i>p</i> -(2-Carboxyethyl)-phenethylamino-5'- <i>N</i> -ethylcarboxamidoadenosine		
KF17837	= ( <i>E</i> )-8-(3,4-dimethoxystyryl)-1,3-dipropyl-7-methylxanthine		
SCH 58261	= 7-(2-Phenylethyl)-5-amino-2-(2-furyl)-pyrazolo[4,3- <i>e</i> ]-1,2,4-		

KF24345 = 3-[1-(6,7-Diethoxy-2-morpholinoquinazolin-4-yl)piperidin-4-yl]-1,6-dimethyl-2,4(1*H*, 3*H*)-quinazolinedione hydrochloride

## REFERENCES

- [1] Palmer, T.M.; Stiles, G.L. *Neuropharmacology*, **1995**, *34*, 683.
- [2] Haas, H.L.; Selbach, O. *Naunyn Schmiedeberg's Arch. Pharmacol.*, **2000**, *362*, 375.
- [3] Dunwiddie, T.V.; Masino, S.A. *Ann. Rev. Neurosci.*, **2001**, *24*, 31.
- [4] Fredholm, B.B.; Ijzerman, A.P.; Jacobson, K.A.; Klotz K.N.; Linden, J. *Pharmacol. Rev.*, **2001**, *53*, 527.
- [5] Feoktistov, I.; Biaggioni, I. *Pharmacol. Rev.*, **1997**, *49*, 381.
- [6] Jacobson, K.A. *Trends Pharmacol. Sci.*, **1998**, *19*, 184.
- [7] Baraldi, P.G.; Cacciari, B.; Romagnoli, R.; Merighi, S.; Varani, K.; Borea, P.A.; Spalluto, G. *Med. Res. Rev.*, **2000**, *20*, 103.
- [8] Fishman, P.; Bar-Yehuda, S. *Curr. Top. Med. Chem.*, **2003**, *3*, 463.
- [9] Phillis, J.W.; Goshgarian, H.G. *Neurol. Res.*, **2001**, *23*, 183.
- [10] Ribeiro, J.A.; Sebastiao, A.M.; de Mendonca, A. *Prog. Neurobiol.*, **2002**, *68*, 377.
- [11] Yan, L.; Burbiel, J.C.; Maass, A.; Muller, C.E. *Expert. Opin. Emerg. Drugs*, **2003**, *8*, 537.
- [12] Boison, D. *Neuroscientist*, **2005**, *11*, 25.
- [13] Xu, K.; Bastia, E.; Schwarzschild, M. *Pharmacol. Ther.*, **2005**, *105*, 267.
- [14] Jacobson, K.A.; Gao, Z.G. *Nat. Rev. Drug Discov.*, **2006**, *5*, 247.
- [15] Thorn, J.A.; Jarvis, S.M. *Adenosine transporters Gen. Pharmacol.*, **1996**, *27*, 613.
- [16] King, A.E.; Ackley, M.A.; Cass, C.E.; Young, J.D.; Baldwin, S.A. *Trends Pharmacol. Sci.*, **2006**, *27*, 416.
- [17] Busatto, G.F.; Pilowsky, L.S. *Br. J. Hosp. Med.*, **1995**, *53*, 309.
- [18] Stoessl, A.J.; Ruth, T.J. *Curr. Opin. Neurol.*, **1998**, *11*, 327.
- [19] Thobois, S.; Guillouet, S.; Broussolle, E. *Neurophysiol. Clin.*, **2001**, *31*, 321.
- [20] Burns, H.D.; Hamill, T.G.; Eng, W.S.; Francis, B.; Fioravanti, C.; Gibson, R.E. *Curr. Opin. Chem. Biol.*, **1999**, *3*, 388.
- [21] Suzuki, F.; Ishiwata, K. *Drug Develop. Res.*, **1998**, *45*, 312.
- [22] Ishiwata, K.; Shimada, J.; Ishii, K.; Suzuki, F. *Drugs Future*, **2002**, *27*, 569.
- [23] Holschbach, M.H.; Olsson, R.A. *Curr. Pharm. Des.*, **2002**, *8*, 2345.
- [24] Fastbom, J.; Pazos, A.; Probst, A.; Palacios, J.M. *Neuroscience*, **1987**, *22*, 827.
- [25] Svenningsson, P.; Hall, H.; Sedvall, G.; Fredholm, B.B. *Synapse*, **1997**, *27*, 322.
- [26] Kull, B.; Svenningsson, P.; Hall, H.; Fredholm, B.B. *Neuropharmacology*, **2000**, *39*, 2374.
- [27] Jennings, L.L.; Hao, C.; Cabrera, M.A.; Vickers, M.F.; Baldwin, S.A.; Young, J.D.; Cass, C.E. *Neuropharmacology*, **2001**, *40*, 722.
- [28] Glass, M.; Faull, R.L.; Dragunow, M. *Brain Res.*, **1996**, *710*, 79.
- [29] Jansen, K.; Faull, R.L.M.; Dragunow, M.; Synek, B.J.L. *Neuroscience*, **1990**, *39*, 613.
- [30] Kaloria, R.N.; Sromek, S.; Wilcox, B.J.; Unnerstall, J.R. *Neurosci. Lett.*, **1990**, *118*, 257.
- [31] Jaarsma, D.; Sebens, J.B.; Korf, J. *Neurosci. Lett.*, **1991**, *121*, 111.
- [32] Ulas, J.; Brunner, L.C.; Nguyen, L.; Cotman, C.W. *Neuroscience*, **1993**, *52*, 843.
- [33] Deckert, J.; Abel, F.; Kunig, G.; Hartmann, J.; Senitz, D.; Maier, H.; Ransmayr, G.; Riederer, P. *Neurosci. Lett.*, **1998**, *244*, 1.
- [34] Ikeda, M.; Mackay, K.B.; Dewar, D.; McCulloch, J. *Brain Res.*, **1993**, *616*, 211.
- [35] Angelatou, F.; Pagonopoulou, O.; Maraziotis, T.; Olivier, A.; Villemure, J.G.; Avoli, M.; Kostopoulos, G. *Neurosci. Lett.*, **1993**, *163*, 11.
- [36] Glass, M.; Faull, R.L.; Bullock, J.Y.; Jansen, K.; Mee, E.W.; Walker, E.B.; Synek, B.J.; Dragunow, M. *Brain Res.*, **1996**, *710*, 56.
- [37] Martinez-Mir, M.I.; Probst, A.; Palacios, J.M. *Neuroscience*, **1991**, *42*, 697.
- [38] Glass, M.; Dragunow, M.; Faull, R.L. *Neuroscience*, **2000**, *97*, 505.
- [39] Kurumaji, A.; Toru, M. *Brain Res.*, **1998**, *808*, 320.
- [40] Deckert, J.; Brenner, M.; Durany, N.; Zochling, R.; Paulus, W.; Ransmayr, G.; Tatschner, T.; Danielczyk, W.; Jellinger, K.; Riederer, P. *Neuroreport*, **2003**, *14*, 313.
- [41] Müller, C.E.; Stein, B. *Curr. Pharmaceut. Design*, **1996**, *2*, 501.
- [42] Poulsen, S.-A.; Quinn, R.J. *Bioorg. Med. Chem.*, **1998**, *6*, 619.
- [43] Müller, C.E. *Curr. Med. Chem.*, **2000**, *7*, 1269.
- [44] Soudijn, W.; van Wijngaarden, I.; IJzerman, A.P. *Curr. Top. Med. Chem.*, **2003**, *3*, 355.
- [45] Dhalla, A.K.; Shryock, J.C.; Shreeniwas, R.; Belardinelli, L. *Curr. Top. Med. Chem.*, **2003**, *3*, 369.
- [46] Bruns, R.F.; Fergus, J.H.; Badger, E.W.; Bristol, J.A.; Santay, L.A.; Hartman, J.D.; Hays, S.J.; Huang, C.C. *Naunyn-Schmiedeberg's Arch. Pharmacol.*, **1987**, *335*, 59.
- [47] Lohse, M.J.; Klotz, K.-N.; Lindenborn-Fotinos, J.; Reddington, M.; Schwabe, U.; Olsson, R.A. *Naunyn-Schmiedeberg's Arch. Pharmacol.*, **1987**, *336*, 204.
- [48] Shimada, J.; Suzuki, F.; Nonaka, H.; Karasawa, A.; Mizumoto, H.; Ohno, T.; Kubo, K.; Ishii, A. *J. Med. Chem.*, **1991**, *34*, 466.
- [49] Suzuki, F.; Shimada, J.; Mizumoto, H.; Karasawa, A.; Kubo, K.; Nonaka, H.; Ishii, A.; Kawakita, T. *J. Med. Chem.*, **1992**, *35*, 3066.
- [50] Kuroda, S.; Takamura, F.; Tenda, Y.; Itani, H.; Tomishima, Y.; Akahane, A.; Sakane, K. *Chem. Pharm. Bull. (Tokyo)*, **2001**, *49*, 988.
- [51] Bissler, J.C.; Pascal, O.; Deckert, J.; Maziere, B. *Brain Res.*, **1992**, *599*, 6.
- [52] Bulicz, J.; Bertarelli, D.C.; Baumert, D.; Fulle, F.; Muller, C.E.; Heber, D. *Bioorg. Med. Chem.*, **2006**, *14*, 2837.
- [53] Ishiwata, K.; Ishii, S.; Shinoda, M.; Maekawa, S.; Senda, M. *Appl. Radiat. Isot.*, **1999**, *50*, 693.
- [54] Ishiwata, K.; Furuta, R.; Shimada, J.; Ishii, S.; Endo, K.; Suzuki, F.; Senda, M. *Appl. Radiat. Isot.*, **1995**, *46*, 1009.
- [55] Furuta, R.; Ishiwata, K.; Kiyosawa, M.; Ishii, S.; Saito, N.; Shimada, J.; Endo, K.; Suzuki, F.; Senda, M. *J. Nucl. Med.*, **1996**, *37*, 1203.
- [56] Noguchi, J.; Ishiwata, K.; Furuta, R.; Simada, J.; Kiyosawa, M.; Ishii, S.; Endo, K.; Suzuki, F.; Senda, M. *Nucl. Med. Biol.*, **1997**, *24*, 53.
- [57] Wakabayashi, S.; Nariai, T.; Ishiwata, K.; Nagaoka, T.; Hirakawa, K.; Oda, K.; Sakiyama, Y.; Shumiya, S.; Toyama, H.; Suzuki, F.; Senda, M. *Nucl. Med. Biol.*, **2000**, *27*, 401.
- [58] Shimada, Y.; Ishiwata, K.; Kiyosawa, M.; Nariai, T.; Oda, K.; Toyama, H.; Suzuki, F.; Ono, K.; Senda, M. *Nucl. Med. Biol.*, **2002**, *29*, 29.
- [59] Kiyosawa, M.; Ishiwata, K.; Noguchi, J.; Endo, K.; Wang, W.F.; Suzuki, F.; Senda, M. *Jpn. J. Ophthalmol.*, **2001**, *45*, 264.
- [60] Nariai, T.; Shimada, Y.; Ishiwata, K.; Nagaoka, T.; Shimada, J.; Kuroiwa, T.; Ono, K.; Hirakawa, K.; Senda, M.; Ohno, K. *Acta Neurochir. Suppl.*, **2003a**, *86*, 45.
- [61] Nariai, T.; Shimada, Y.; Ishiwata, K.; Nagaoka, T.; Shimada, J.; Kuroiwa, T.; Ono, K.; Ohno, K.; Hirakawa, K.; Senda, M. *J. Nucl. Med.*, **2003b**, *44*, 1839.
- [62] Ishiwata, K.; Nariai, T.; Kimura, Y.; Oda, K.; Kawamura, K.; Ishii, K.; Senda, M.; Wakabayashi, S.; Shimada, Y. *J. Ann. Nucl. Med.*, **2002**, *16*, 377.
- [63] Holschbach, M.H.; Fein, T.; Krummeich, C.; Lewis, R.G.; Wutz, W.; Schwabe, U.; Unterlugauer, D.; Olsson, R.A. *J. Med. Chem.*, **1998**, *41*, 555.
- [64] Holschbach, M.H.; Olsson, R.A.; Bier, D.; Wutz, W.; Sihver, W.; Schuller, M.; Palm, B.; Coenen, H.H. *J. Med. Chem.*, **2002**, *45*, 5150.
- [65] Bauer, A.; Langen, K.J.; Bidmon, H.; Holschbach, M.H.; Weber, S.; Olsson, R.A.; Coenen, H.H.; Zilles, K. *J. Nucl. Med.*, **2005**, *46*, 450.
- [66] Meyer, P.T.; Bier, D.; Holschbach, M.H.; Cremer, M.; Tellmann, L.; Bauer, A. *Eur. J. Nucl. Med. Mol. Imaging*, **2003**, *30*, 1440.
- [67] Matsuya, T.; Takamatsu, H.; Murakami, Y.; Noda, A.; Ichise, R.; Awaga, Y.; Nishimura, S. *Nucl. Med. Biol.*, **2005**, *32*, 837.
- [68] Blum, T.; Ermert, J.; Wutz, W.; Bier, D.; Coenen, H.H. *J. Label. Compd. Radiopharm.*, **2004**, *47*, 415.
- [69] Bauer, A.; Holschbach, M.H.; Meyer, P.T.; Boy, C.; Herzog, H.; Olsson, R.A.; Coenen, H.H.; Zilles, K. *NeuroImage*, **2003**, *19*, 1760.
- [70] Fukumitsu, N.; Ishii, K.; Kimura, K.; Oda, K.; Sasaki, T.; Mori, Y.; Ishiwata, K. *Ann. Nucl. Med.*, **2003**, *17*, 511.
- [71] Fukumitsu, N.; Ishii, K.; Kimura, K.; Oda, K.; Sasaki, T.; Mori, Y.; Ishiwata, K. *J. Nucl. Med.*, **2005**, *46*, 32.
- [72] Meyer, P.T.; Elmenhorst, D.; Matusch, A.; Bauer, A. *NeuroImage*, **2006**, *32*, 1100.
- [73] Bier, D.; Holschbach, M.H.; Wutz, W.; Olsson, R.A.; Coenen, H.H. *Drug. Metab. Dispos.*, **2006**, *34*, 570.

- [74] Kimura, Y.; Ishii, K.; Fukumitsu, N.; Oda, K.; Sasaki, T.; Kawamura, K.; Ishiwata, K. *Nucl. Med. Biol.*, **2004**, *31*, 975.
- [75] Meyer, P.T.; Bier, D.; Holschbach, H.; Boy, C.; Olsson, R.A.; Coenen, H.H.; Zilles, K.; Bauer, A. *J. Cereb. Blood Flow Metab.*, **2004**, *24*, 323.
- [76] Meyer, P.T.; Elmenhorst, D.; Bier, D.; Holschbach, M.H.; Matusch, A.; Coenen, H.H.; Zilles, K.; Bauer, A. *NeuroImage*, **2005**, *24*, 1192.
- [77] Naganawa, M.; Kimura, Y.; Nariai, T.; Ishii, K.; Oda, K.; Manabe, Y.; Chihara, K.; Ishiwata, K. *NeuroImage*, **2005**, *26*, 885.
- [78] Meyer, P.T.; Elmenhorst, D.; Zilles, K.; Bauer, A. *Synapse*, **2005**, *55*, 212.
- [79] Koeppe, R.A.; Holthoff, V.A.; Frey, K.A.; Kilbourn, M.R.; Kuhl, D.E. *J. Cereb. Blood Flow Metab.*, **1991**, *11*, 735.
- [80] Mintun, M.A.; Raichle, M.E.; Kilbourn, M.R.; Wooten, G.F.; Welch, M.J. *Ann. Neurol.*, **1984**, *15*, 217.
- [81] Logan, J.; Fowler, J.S.; Volkow, N.D.; Wolf, A.P.; Dewey, S.L.; Schlyer, D.J.; MacGregor, R.R.; Hitzmann, R.; Bendriem, B.; Gately, S.J.; Christman, D.R. *J. Cereb. Blood Flow Metab.*, **1990**, *10*, 740.
- [82] Logan, J. *Nucl. Med. Biol.*, **2000**, *27*, 661.
- [83] Rehfeldt, K.H.; Sanders, M.S. *Anesth. Analg.*, **2000**, *90*, 45.
- [84] Jons, P.H.; Ernst, M.; Hankerson, J.; Hardy, J.; Zametkin, A.J. *Human Brain Map.*, **1997**, *5*, 119.
- [85] Logan, J.; Fowler, J.S.; Volkow, N.D.; Wang, G.-J.; Ding, Y.-S.; Alexoff, D.L. *J. Cereb. Blood Flow Metab.*, **1996**, *16*, 834.
- [86] Gunn, R.N.; Lammertsma, A.A.; Hume, S.P.; Cunningham, V.J. *NeuroImage*, **1997**, *6*, 279.
- [87] Naganawa, M.; Kimura, Y.; Ishii, K.; Oda, K.; Ishiwata, K.; Matani, A. *IEEE Trans. Biomed. Eng.*, **2005**, *52*, 201.
- [88] Hwang, D.R.; Simpson, N.R.; Montoya, J.; Man, J.J.; Laruelle, M. *Nucl. Med. Biol.*, **1999**, *26*, 815.
- [89] Morrison, C.F.; Elzein, E.; Jiang, B.; Ibrahim, P.N.; Marquart, T.; Palle, V.; Shenk, K.D.; Varkhedkar, V.; Maa, T.; Wu, L.; Wu, Y.; Zeng, D.; Fong, I.; Lustig, D.; Leung, K.; Zablocki, J.A. *Bioorg. Med. Chem. Lett.*, **2004**, *14*, 3793.
- [90] Franchetti, P.; Cappellacci, L.; Marchetti, S.; Trincavelli, L.; Martini, C.; Mazzoni, M.R.; Lucacchini, A.; Grifantini, M. *J. Med. Chem.*, **1998**, *41*, 1708.
- [91] Beukers, M.W.; Wanner, M.J.; Von Frijtag Drabbe Kunzel, J.K.; Klaasse, E.C.; IJzerman, A.P.; Koomen, G.J. *J. Med. Chem.*, **2003**, *46*, 1492.
- [92] Chang, L.C.; Spanjersberg, R.F.; Von Frijtag Drabbe Kunzel, J.K.; Mulder-Krieger, T.; van den Hout, G.; Beukers, M.W.; Brussee, J.; IJzerman, A.P. *J. Med. Chem.*, **2004**, *47*, 6529.
- [93] Baraldi, P.G.; Pavani, M.G.; Leung, E.; Moorman, A.R.; Varani, K.; Vincenzi, F.; Borea, P.A.; Romagnoli, R. *Bioorg. Med. Chem. Lett.*, **2006**, *16*, 1402.
- [94] Baraldi, P.G.; Romagnoli, R.; Pavani, M.G.; Nunez Mdel, C.; Tabrizi, M.A.; Shryock, J.C.; Leung, E.; Moorman, A.R.; Uluoglu, C.; Iannotta, V.; Merighi, S.; Borea, P.A. *J. Med. Chem.*, **2003**, *46*, 794.
- [95] de Ligt, R.A.; van der Klein, P.A.; Von Frijtag Drabbe Kunzel, J.K.; Lorenzen, A.; Ait, E.I.; Maate, F.; Fujikawa, S.; van Westhoven, R.; van den Hoven, T.; Brussee, J.; IJzerman, A.P. *Bioorg. Med. Chem.*, **2004**, *12*, 139.
- [96] Chordia, M.D.; Zigler, M.; Murphree, L.J.; Figler, H.; Macdonald, T.L.; Olsson, R.A.; Linden, J. *J. Med. Chem.*, **2005**, *48*, 5131.
- [97] Seale, T.W.; Abla, K.A.; Shamim, M.T.; Carney, J.M.; Daly, J.W. *Life Sci.*, **1988**, *43*, 1671.
- [98] Shimada, J.; Suzuki, J.; Nonaka, H.; Ishii, A.; Ichikawa, S. *J. Med. Chem.*, **1992**, *35*, 2342.
- [99] Nonaka, H.; Ichimura, M.; Takeda, M.; Nonaka, Y.; Shimada, J.; Suzuki, F.; Yamakuchi, K.; Kase, A. *Eur. J. Pharmacol.*, **1994a**, *267*, 335.
- [100] Francis, J.E.; Cash, W.D.; Psychoyos, G.; Ghai, G.; Wenk, P.; Friedman, R.C.; Atkins, C.; Warren, V.; Furness, P.; Huyn, J.L.; Stone, G.A.; Desai, M.; Williams, M. *J. Med. Chem.*, **1988**, *31*, 1014.
- [101] Baraldi, P.G.; Cacciari, B.; Spalluto, G.; Borioni, A.; Viziano, M.; Dionisotti, S.; Ongini, E. *Curr. Med. Chem.*, **1995**, *2*, 722.
- [102] Cristalli, G.; Lambertucci, C.; Taffi, S.; Vittori, S.; Volpini, R. *Curr. Top. Med. Chem.*, **2003**, *3*, 387.
- [103] Nonaka, H.; Mori, A.; Ichimura, M.; Shindou, T.; Yanagawa, K.; Shimada, J.; Kase, H. *Mol. Pharmacol.*, **1994b**, *46*, 817.
- [104] Zocchi, C.; Ongini, E.; Ferrara, S.; Baraldi, P.G.; Dionisotti, S. *Br. J. Pharmacol.*, **1996**, *117*, 1381.
- [105] Fredholm, B.B.; Lindstrom, K.; Dionisotti, S.; Ongini, E. *J. Neurochem.*, **1998**, *70*, 1210.
- [106] Alexander, S.P.; Millns, P. *J. Eur. J. Pharmacol.*, **2001**, *411*, 205.
- [107] DeMet, E.M.; Chicz-DeMet, A. *Naunyn-Schmiedeberg's Arch. Pharmacol.*, **2002**, *366*, 478.
- [108] Ishiwata, K.; Noguchi, J.; Toyama, H.; Sakiyama, Y.; Koike, N.; Ishii, S.; Oda, K.; Endo, K.; Suzuki, F.; Senda, M. *Appl. Radiat. Isot.*, **1996**, *47*, 507.
- [109] Stone-Elander, S.; Thorell, J.O.; Eriksson, L.; Fredholm, B.B.; Ingvar, M. *Nucl. Med. Biol.*, **1997**, *24*, 187.
- [110] Noguchi, J.; Ishiwata, K.; Wakabayashi, S.; Nariai, T.; Shumiya, S.; Ishii, S.; Toyama, H.; Endo, K.; Suzuki, F.; Senda, M. *J. Nucl. Med.*, **1998**, *39*, 498.
- [111] Ishiwata, K.; Noguchi, J.; Wakabayashi, S.; Shimada, J.; Ogi, N.; Nariai, T.; Tanaka, A.; Endo, K.; Suzuki, F.; Senda, M. *J. Nucl. Med.*, **2000a**, *41*, 345.
- [112] Marian, T.; Boros, I.; Lengyel, Z.; Balkay, L.; Horvath, G.; Emri, M.; Sarkadi, E.; Szentmiklosi, A.J.; Fekete, I.; Tron, L. *Appl. Radiat. Isot.*, **1999**, *50*, 887.
- [113] Ishiwata, K.; Ogi, N.; Shimada, J.; Nonaka, H.; Tanaka, A.; Suzuki, F.; Senda, M. *Ann. Nucl. Med.*, **2000b**, *14*, 81.
- [114] Cunha, R.A.; Johansson, B.; Constantino, M.D.; Sebastião, A.M.; Fredholm, B.B. *Naunyn-Schmiedeberg's Arch. Pharmacol.*, **1996**, *353*, 261.
- [115] Lindstrom, K.; Ongini, E.; Fredholm, B.B. *Naunyn-Schmiedeberg's Arch. Pharmacol.*, **1996**, *354*, 539.
- [116] Ishiwata, K.; Ogi, N.; Hayakawa, N.; Oda, K.; Nagaoka, T.; Toyama, H.; Suzuki, F.; Endo, K.; Tanaka, A.; Senda, M. *Ann. Nucl. Med.*, **2002**, *16*, 467.
- [117] Ishiwata, K.; Ogi, N.; Shimada, J.; Wang, W.; Ishii, K.; Tanaka, A.; Suzuki, F.; Senda, M. *Ann. Nucl. Med.*, **2000c**, *14*, 461.
- [118] Ishiwata, K.; Wang, W.F.; Kimura, Y.; Kawamura, K.; Ishii, K. *Ann. Nucl. Med.*, **2003**, *17*, 205.
- [119] Ishiwata, K.; Shimada, J.; Wang, W.F.; Harakawa, H.; Ishii, S.; Kiyosawa, M.; Suzuki, F.; Senda, M. *Ann. Nucl. Med.*, **2000d**, *14*, 247.
- [120] Müller, C.E.; Geis, U.; Hipp, J.; Schobert, U.; Frobenius, W.; Pawlowski, M.; Suzuki, F.; Sandoval-Ramírez, J. *J. Med. Chem.*, **1997**, *40*, 4396.
- [121] Müller, C.E.; Sandoval-Ramírez, J.; Schobert, U.; Geis, U.; Frobenius, W.; Klotz, K.N. *Bioorg. Med. Chem.*, **1998**, *6*, 707.
- [122] Wang, W.F.; Ishiwata, K.; Nonaka, H.; Ishii, S.; Kiyosawa, M.; Shimada, J.; Suzuki, F.; Senda, M. *Nucl. Med. Biol.*, **2000**, *27*, 541.
- [123] Hirani, E.; Gillies, J.; Karasawa, A.; Shimada, J.; Kase, H.; Opacka-Juffry, J.; Osman, S.; Luthra, S.K.; Hume, S.P.; Brooks, D.J. *Synapse*, **2001**, *42*, 164.
- [124] Shimada, J.; Koike, N.; Nonaka, H.; Shiozaki, S.; Yanagawa, K.; Kanda, T.; Kobayashi, H.; Ichimura, M.; Nakamura, J.; Kase, H.; Suzuki, F. *Bio. Med. Chem. Lett.*, **1997**, *7*, 2349.
- [125] Kase, H. *Biosci. Biotechnol. Biochem.*, **2001**, *65*, 1447.
- [126] Bara-Jimenez, W.; Sherzai, A.; Dimitrova, T.; Favit, A.; Bibbiani, F.; Gillespie, M.; Morris, M.J.; Mouradian, M.M.; Chase, T.N. *Neurology*, **2003**, *61*, 293.
- [127] Hauser, R.A.; Hubble, J.P.; Truong, D.D. *Neurology*, **2003**, *61*, 297.
- [128] Kawamura, K.; Ishiwata, K. *Ann. Nucl. Med.*, **2004**, *18*, 165.
- [129] Nonaka, Y.; Shimada, J.; Nonaka, H.; Koike, N.; Aoki, N.; Kobayashi, H.; Kase, H.; Yamaguchi, K.; Suzuki, F. *J. Med. Chem.*, **1993**, *36*, 3731.
- [130] Todde, S.; Moresco, R.M.; Simonelli, P.; Baraldi, P.G.; Cacciari, B.; Spalluto, G.; Varani, K.; Monopoli, A.; Matarrese, M.; Carpinelli, A.; Magni, F.; Kienle, M.G.; Fazio, F. *J. Med. Chem.*, **2000**, *43*, 4359.
- [131] Moresco, R.M.; Todde, S.; Belloli, S.; Simonelli, P.; Panzacchi, A.; Rigamonti, M.; Galli-Kienle, M.; Fazio, F. *Eur. J. Nucl. Med. Mol. Imaging*, **2005**, *32*, 405.
- [132] Ishiwata, K.; Mishina, M.; Kimura, Y.; Oda, K.; Sasaki, T.; Ishii, K. *Synapse*, **2005**, *55*, 133.
- [133] Naganawa, M.; Kimura, Y.; Mishina, M.; Manabe, Y.; Chihara, K.; Oda, K.; Ishii, K.; Ishiwata, K. *Euro J Nucl Med Mol Imaging*, **2006**, DOI. 10.1007/s00259-006-0294-0.
- [134] Fredholm, B.B.; Svenningsson, P. *Neurology*, **2003**, *61*, S5.
- [135] Holschbach, M.H.; Bier, D.; Wutz, W.; Sihver, W.; Schuller, M.; Olsson, R.A. *Eur. J. Med. Chem.*, **2005**, *40*, 421.
- [136] Holschbach, M.H.; Bier, D.; Stusgen, S.; Wutz, W.; Sihver, W.;

- Coenen, H.H.; Olsson, R.A. *Eur. J. Med. Chem.*, **2006**, *41*, 7.
- [137] Minetti, P.; Tinti, M.O.; Carminati, P.; Castorina, M.; Di Cesare M.A.; Di Serio, S.; Gallo, G.; Ghirardi, O.; Giorgi, F.; Giorgi, L.; Piersanti, G.; Bartocchini, F.; Tarzia, G. *J. Med. Chem.*, **2005**, *48*, 6887.
- [138] Peng, H.; Kumaravel, G.; Yao, G.; Sha L.; Wang J., van Vlijmen, H.; Bohnert, T.; Huang, C.; Vu C.B.; Ensinger, C.L.; Chang H.; Engber, T.M.; Whalley, E.T.; Petter R.C. *J. Med. Chem.*, **2004**, *47*, 6218.
- [139] Vu, C.B.; Shields, P.; Peng, B.; Kumaravel, G.; Jin, X.; Phadke, D.; Wang, J.; Engber, T.; Ayyub, E.; Petter, R.C. *Bioorg. Med. Chem. Lett.*, **2004**, *14*, 4835.
- [140] Vu, C.B.; Pan, D.; Peng, B.; Kumaravel, G.; Smits, G.; Jin, X.; Phadke, D.; Engber, T.; Hunag, C.; Reilly, J.; Tam, S.; Grant, D.; Hetu, D.; Petter, R.C. *J. Med. Chem.*, **2005**, *48*, 2009.
- [141] Matasi, J.J.; Caldwell, J.P.; Hao, J.; Neustadt, B.; Arik L.; Foster, C.J.; Lachowicz, J.; Tulshian, D.B. *Bioorg. Med. Chem. Lett.*, **2005**, *15*, 1333.
- [142] Matasi, J.J.; Caldwell, J.P.; Zhang, H.; Fawzi, A.; Cohen-Williams, M.E.; Varty, G.B.; Tulshian, D.B. *Bioorg. Med. Chem. Lett.*, **2005**, *15*, 3670.
- [143] Feoktistov, I.; Ryzhov, S.; Goldstein, A.E.; Biaggioni, I. *Circ. Res.*, **2003**, *92*, 485.
- [144] Ilas, J.; Pecar, S.; Hockemeyer, J.; Euler, H.; Kirfel, A.; Mueller, C.E. *J. Med. Chem.*, **2005**, *48*, 2108.
- [145] Ji, X.; Kim, Y.C.; Ahern, D.G.; Linden J.; Jacobson, K.A. *Biochem. Pharmacol.*, **2001**, *61*, 657
- [146] Baraldi, P.G.; Tabrizi, M.A.; Preti, D.; Bovero, A.; Fruttarolo, F.; Romagnoli, R.; Moorman, A.R.; Gessi, S.; Merighi, S.; Varani, K.; Borea, P.A. *Bioorg. Med. Chem. Lett.*, **2004**, *14*, 3606.
- [147] Salvatore, C.A.; Jacobson, M.A.; Taylor, H.E.; Linden, J.; Johnson, R.G. *Proc. Natl. Acad. Sci. U.S.A.*, **1993**, *90*, 10365.
- [148] Von Lubitz, D.K.; Lin, R.C.; Popik, P.; Carter, M.F.; Jacobson, K.A. *Eur. J. Pharmacol.*, **1994**, *263*, 59.
- [149] van Calker, D.; Biber, K. *Neurochem. Res.*, **2005**, *30*, 1205.
- [150] Fedorova, I.M.; Jacobson, M.A.; Basile, A.; Jacobson, K.A. *Cell Mol. Neurobiol.*, **2003**, *23*, 431.
- [151] DeNinno, M.P.; Masamune, H.; Chenard, L.K.; DiRico, K.J.; Eller, C.; Etienne, J.B.; Tickner, J.E.; Kennedy, S.P.; Knight, D.R.; Kong, J.; Oleynek, J.J.; Tracey, W.R.; Hill, R. *J. Med. Chem.*, **2003**, *46*, 353.
- [152] Jeong, L.S.; Lee, H.W.; Jacobson, K.A.; Kim, H.O.; Shin, D.H.; Lee, J.A.; Gao, Z.G.; Lu, C.; Duong, H.T.; Gunaga, P.; Lee, S.;K.; Jin, D.Z.; Chun, M.W.; Moon, H.R. *J. Med. Chem.*, **2006**, *49*, 273.
- [153] Tchilibon, S.; Joshi, B.V.; Kim, S.K.; Duong, H.T.; Gao, Z. G.; Jacobson, K.A. *J. Med. Chem.*, **2005**, *48*, 1745.
- [154] Pastorin, G.; Da Ros, T.; Bolcato, C.; Montopoli, C.; Moro, S.; Cacciari, B.; Baraldi, P.G.; Varani, K.; Borea, P.A.; Spalluto, G. *J. Med. Chem.*, **2006**, *49*, 1720.
- [155] Okamura, T.; Kurogi, Y.; Nishikawa, H.; Hashimoto, K.; Fujiwara, H.; Nagao, Y. *J. Med. Chem.*, **2002**, *45*, 3703.
- [156] Müller, C.E.; Thorand, M.; Qurishi, R.; Diekmann, M.; Jacobson, K.A.; Padgett, W.L.; Daly, J.W. *J. Med. Chem.*, **2002a**, *45*, 3440.
- [157] Müller, C.E.; Diekmann, M.; Thorand, M.; Ozola, V. *Bioorg. Med. Chem. Lett.*, **2002b**, *12*, 501.
- [158] Colotta, V.; Catarzi, D.; Varano, F.; Cecchi, L.; Filacchioni, G.; Martini, C.; Trincavelli, L.; Lucacchini, A. *J. Med. Chem.*, **2000**, *43*, 3118.
- [159] Colotta, V.; Catarzi, D.; Varano, F.; Calabri, F.R.; Lenzi, O.; Filacchioni, G.; Martini, C.; Trincavelli, L.; Deflorian, F.; Moro, S. *J. Med. Chem.*, **2004**, *47*, 3580.
- [160] Muijlwijk-Koezen, J. E.; Timmerman, H.; van der Goot, H.; Mengge, W. M.; Frijtag Von Drabbe, Kunzel, J., de Groot, M., IJzerman, A. P. *J. Med. Chem.*, **2000**, *43*, 2227.
- [161] Jung, K.Y.; Kim, S. K.; Gao, Z.G.; Gross, A.S.; Melman, N.; Jacobson, K. A.; Kim, Y.C. *Bioorg. Med. Chem.*, **2004**, *12*, 613.
- [162] Li, A.H.; Moro, S.; Forsyth, N.; Melman, N.; Ji, X.D.; Jacobson, K.A. *J. Med. Chem.*, **1999a**, *42*, 706.
- [163] Li, A.H.; Chang, L.; Ji, X.; Melman, N.; Jacobson, K.A. *Bioconjug. Chem.*, **1999b**, *10*, 667.
- [164] Gao, Z.G.; Muijlwijk-Koezen, J.E.; Chen, A.; Muller, C.E.; IJzerman, A.P.; Jacobson, K.A. *Mol. Pharmacol.*, **2001**, *60*, 1057.
- [165] Göblyös, A.; Gao, Z.G.; Brussee, J.; Connestari, R.; Santiago, S.N.; Ye, K.; IJzerman, A.P.; Jacobson, K.A. *J. Med. Chem.*, **2006**, *49*, 3354.
- [166] King, A.E.; Ackley, M.A.; Cass, C.E.; Young, J.D.; Baldwin, S.A. *Trends Pharmacol. Sci.*, **2006**, *27*, 416.
- [167] Ishiwata, K.; Takai, H.; Nonaka, H.; Ishii, S.; Shimada, J.; Senda, M. *Nucl. Med. Biol.*, **2001**, *28*, 281.
- [168] Mathews, W.B.; Nakamoto, Y.; Abraham, E.H.; Scheffel, U.; Hilton, J.; Ravert, H.T.; Tatsumi, M.; Rauseo, P.A.; Traughber, B.J.; Salikhova, A.Y.; Dannals, R.F.; Wahl, R.L. *Mol. Imaging Biol.*, **2005**, *7*, 203.
- [169] Hammond, J.R.; Archer, R.G.E. *J. Pharmacol. Exp. Ther.*, **2004**, *308*, 1083.
- [170] Tromp, R.A.; Spanjersberg, R.F.; von Frijtag Drabbe Kuenzel, J.K.; IJzerman, A.P. *J. Med. Chem.*, **2005**, *48*, 321.
- [171] Gupte A., Buolamwini J.K. *Bioorg. Med. Chem. Lett.*, **2004**, *14*, 2257.
- [172] Sasamori, J.; Aihara, K.; Yoneyama, F.; Sato, I.; Kogi, K.; Takeo, S. *Vasc. Pharmacol.*, **2006**, *47*, 614.
- [173] Massip, S.; Guillon, J.; Bertarelli, D.; Bosc, J.J.; Leger, J.M.; Lacher, S.; Bontemps, C.; Dupont, T.; Mueller, C.E.; Jarry, C. *Bioorg. Med. Chem.*, **2006**, *14*, 2697.
- [174] Stewart, M.; Steini, A.G.; Ma, C.; Song, J.P.; McKibben, B.; Castellano, A.L.; MacLennan, S.J. *Biochem. Pharmacol.*, **2004**, *68*, 305.
- [175] Kalla, R.V.; Elzein, E.; Perry, T.; Li X.; Palle, V.; Varkhedkar, V.; Gimbel, A.; Maa, T.; Zeng, D.; Zablocki, J. *J. Med. Chem.*, **2006**, *49*, 3682.
- [176] Kalla, R.V.; Elzein, E.; Perry, T.; Li X.; Palle, V.; Varkhedkar, V.; Gimbel, A.; Maa, T.; Zeng, D.; Zablocki, J. *J. Med. Chem.*, **2006**, *49*, 3682.